



HAL
open science

Effect of the pendent groups on biobased polymers, obtained from click chemistry suitable, for the adsorption of organic pollutants from water

Nour El Houda Birimi, Taha Chabbah, Saber Chatti, Frédéric Schiets, Hervé Casabianca, C. Marestin, Regis Mercier, Steffen Weidner, Abdelhamid Errachid, Nicole Jaffrezic-Renault, et al.

► To cite this version:

Nour El Houda Birimi, Taha Chabbah, Saber Chatti, Frédéric Schiets, Hervé Casabianca, et al.. Effect of the pendent groups on biobased polymers, obtained from click chemistry suitable, for the adsorption of organic pollutants from water. *Polymers for Advanced Technologies*, In press, 10.1002/pat.5809 . hal-03769693

HAL Id: hal-03769693

<https://hal.science/hal-03769693>

Submitted on 5 Sep 2022

HAL is a multi-disciplinary open access archive for the deposit and dissemination of scientific research documents, whether they are published or not. The documents may come from teaching and research institutions in France or abroad, or from public or private research centers.

L'archive ouverte pluridisciplinaire **HAL**, est destinée au dépôt et à la diffusion de documents scientifiques de niveau recherche, publiés ou non, émanant des établissements d'enseignement et de recherche français ou étrangers, des laboratoires publics ou privés.

Effect of the pendent groups on biobased polymers, obtained from click chemistry suitable, for the adsorption of organic pollutants from water

Nour El Houda Brirmi^{1,4}, Taha Chabbah^{1,4}, Saber Chatti¹, Frédéric Schiets², Hervé Casabianca², Catherine Marestin³, Regis Mercier³, Steffen M. Weidner⁵, Abdelhamid Errachid², Nicole Jaffrezic-Renault^{2*}, Hatem Ben Romdhane⁴.

¹National Institute of Research and Physicochemical Analysis (INRAP), Biotechnopole of SidiThabet, 2020 Ariana, Tunisia

² University of Lyon, Institute of Analytical Sciences, UMR 5280, 5 Rue de la Doua, 69100 Villeurbanne, France

³University of Lyon, Institute of Polymer Materials IMP-INSA, UMR 5223, F-69621, Villeurbanne Cedex, France

⁴University of Tunis El Manar, Faculty of Sciences, Farhat Hached University campus, 1068 Tunis, Tunisia

⁵BAM, Federal Institute of Material Research and Testing, Richard Willstätter Str. 11, D-12489 Berlin

Abstract:

In this work, four triazole-based poly(ether-pyridine)s polymers were synthesized and used as an adsorbent for the removal of phenolic compounds from aqueous solutions. For this purpose, new fluoromonomers containing 1,2,3-triazole units were prepared by the Cu(I)-catalyzed 1,3-dipolar cycloaddition reaction and then used for the elaboration of novel poly(ether-pyridine-triazole)s (PEPTs) by direct polycondensation with isosorbide and bisphenol A. Chemical structure of fluorinated pyridinic monomers as well as resulting polymers was confirmed by ¹H and ¹⁹F NMR spectroscopic methods. The thermal behaviour of the obtained PEPTs was characterized using differential scanning calorimetry (DSC) and thermogravimetric analysis (TGA). Results of sorption showed that polymers can be effectively used as a sorbent for the removal of polar organic pollutants. The isosorbide-based poly(ether-pyridine-triazole) which contains hydrophilic hydroxyl groups as pendants chains (P4) exhibited the highest sorption efficiencies (78-100% after 1 h). In order to explain the results an adsorption mechanism mainly based on π - π interactions and hydrogen bonding with the pendent groups is proposed.

Keywords: biobased polymers, cycloaddition, pentafluoropyridine, adsorption, phenolic compounds

Introduction

The increasing contamination worldwide of aquatic ecosystems with thousands of industrial chemical compounds is one of the most significant environmental problems facing humanity. Organic micro-pollutants such as pesticides, substituted phenols, benzene derivatives and pharmaceuticals are considered major threats to water quality. These toxic molecules are not biodegradable and thus tend to persist in both surface^{1,2} and groundwater sources³⁻⁵, causing severe health problems in humans and in other organisms in the environment⁶⁻¹⁰. For the removal of these contaminants from wastewater, different treatment methods¹¹⁻¹⁶ involving chemical (oxidative processes, Fenton's reagent, photochemical and electrochemical techniques), physical (adsorption, membranes processes) and biological treatments (microbial cultures, fungal degradation) have been used. Among these numerous techniques for water

decontamination, adsorption is the most efficient and popular method for pollutant removal¹⁷. For instance, activated carbon is the most widely used adsorbent material to eliminate organic pollutants from water. However, its ability to purify the water is comprised by several limitations, including its rather expensive production, slow pollutant uptake^{18,19} and poor removal of many hydrophilic micropollutants²⁰. Furthermore, activated carbon is difficultly regenerated requiring high energy^{21,22} (heating to 500–900°C) with loss in performance (10 to 15% loss of adsorbent and adsorption capacity)²³. Therefore, many studies have been undertaken for the development of inexpensive and more effective adsorbent phases based on polysaccharide derivatives such as chitin²⁴⁻²⁶, starch²⁷⁻²⁹, chitosan^{30,31} and cyclodextrin³²⁻³⁴. The sorption onto these natural polymers has received increasing attention because of their particular characteristics (easily available, renewable and biodegradable resources) and properties such as their chemical stability, high reactivity and excellent selectivity towards aromatic compounds and metals. Despite their numerous advantages these materials can suffer from some drawbacks like the insolubility due to the high degrees of cross-linking and the selectivity toward hydrophobic pollutants, they are also not efficient to remove simultaneously various organic pollutants present in water at low concentration (>0.1 mmol/L)^{35,36}. The limited removal of hydrophilic pollutants from water have led researchers to find alternative adsorbent phases that are able to efficiently eliminate these pollutants.

In the present work, we are interested to create new aromatic polymers that are partially biosourced for high adsorption efficiency of organic micropollutants. Since, the synthesis of polymeric materials based on monomers derived from renewable feedstock has attracted a growing attention nowadays because not only of the abundance of these sustainable resources, but also of their possibility to limit environmental issues and the depletion of petroleum resources.³⁷ Among the important biobased byproducts are the 1,4-3,6-dianhydrohexitols existed under three isomers, depending on the positions of their two hydroxyl groups, isosorbide, isomannide, or isoidide. These sugar-based diols were identified as the most useful biosourced monomers for high performance polymers due to their rigid structure, non toxicity, chirality, as well as biodegradability. Thus, a large variety of dianhydrohexitol-based materials, that is, polyesters^{38,39}, polyethers^{40,41}, polyamides^{42,43}, polycarbonates^{44,45}, polytriazoles^{46,47} and polyethersulfones^{48,49} has been generated and characterized. These polymers presented promising high glass transitions, excellent thermal stabilities, and interesting physical properties. Another useful and interesting property has been shown, in the class of poly(ethersulfone)s⁴⁸, is their higher polarity and hydrophilicity compared to bisphenol-A based poly(ether sulfone)s.

Research efforts are therefore underway to take advantage of these properties to study the ability of biobased polymers to remove environmentally toxic pollutants from aqueous media. Recently, Chatti et al.⁵⁰ have reported the use of poly(ether-sulfone)s derived from dianhydrohexitols as adsorbents for a large variety of chemical compounds. They demonstrated that isosorbide based- polymers can be useful as alternative adsorbent to remove contaminants from water. In order to enhance the isosorbide adsorption capacities, Gomri et al.⁵¹ incorporated a perfluoro heterocyclic unit in the polyether backbone, since heterocycles are among the interesting chemical structures to modify the properties of polymers because they usually impart excellent thermal stability with improved solubility. The introduced heteroatomic ring consists on pentafluoropyridine. The combination of this fluorinated pyridine and dianhydrohexitols led

to materials with good flexibility and high hydrophilicity which improved their adsorption efficiency towards polar organic pollutants.

Continuing with our line of research, we have working herein on the development of novel partially biosourced poly(ether-pyridine)s with new design, enhanced thermal properties and higher pollutants uptake. In this process, we have investigated the introduction of a second heterocycle moiety in the lateral chain of poly(ether-pyridine)s. Among the various structures of heterocycles we have chosen the 1,2,3-triazole group due to its rigidity and its stability under a variety of conditions, that it cannot be oxidised or reduced and the fact that triazole ring is a mild Lewis base and the nitrogen atoms can act as hydrogen bond acceptors⁵² which open the possibility of bonding with polar compounds. Furthermore, it was reported that the presence of 1,2,4 or 1,2,3-triazole units in the main chain increases the chemical stability, the mechanical and thermal properties of the resulting polymers as well as the hydrophilicity, necessary to extract organic molecules from water media, giving then rise to materials with high affinity towards the polar micropollutants in aqueous solutions.

In this context, several studies were conducted in introducing 1,2,4 triazole moieties in the main chain of aromatic polymers including polyamides⁵³, polyimides⁵⁴ and poly(amide-imide)s⁵⁵ for the elimination of metallic ions such as Cr^{III}, Co^{II}, Zn^{II}, Pb^{II}, Cd^{II}, Hg^{II}, Mn^{II} and Cr^{VI} as Cr₂O₇²⁻ from aqueous solutions. The results show that triazole groups were found to be efficient chelating units for ions thus made polymers effective solid adsorbent phases in the extraction of cations especially Hg^{II} and anions from water media. As a consequent, the inclusion of 1,2,3-triazole units into macromolecular chains allowed the generation of a series of novel poly(ether-pyridine-triazole)s with improved adsorption capacity. In this study, polyethers bearing pyridine and triazole moieties in the main chain and lateral structure, respectively, are obtained by polycondensation of new 1,2,3-triazole-containing fluorinated monomers with diols. These kind of monomers are synthesized, starting from pentafluoropyridine, via the copper (I) catalyzed azide-alkyne cycloaddition reaction (CuAAC) which is the most studied and reliable click reaction.^{56,57} To the best of our knowledge, the copper will be removed much more efficiently from triazole-containing monomers than from polytriazoles made by CuAAC polyaddition⁵⁸.

On the other hand, our approach relies upon the fact that pentafluoropyridine is highly electrophilic due to the presence of five electronegative fluorine atoms attached to the ring. Thus, all fluorine atoms may be substituted by various nucleophiles to provide a wide range of polyfunctional pyridine derivatives. It is well-established that the nucleophilic attack on pentafluoropyridine is regioselective following this order; 4 (*Para*)-fluorine > 2 (*Ortho*)-fluorine > 3 (*Meta*) fluorine so the reaction with nucleophiles in stoichiometric amounts is selectively at the 4- position.^{59,60} However, a few documented examples have been reported on the exploitation of the regioselectivity of nucleophilic substitution of pentafluoropyridine towards preparing monomers for polymer, dendritic, or network architectures. So we will synthesize partially fluorinated aromatic compounds from perfluoropyridine to serve as attractive monomers for high performance materials. The adsorption efficiency of the new developed polymers to remove hydrophobic and hydrophilic organic micropollutants from aqueous media is determined. The studied organic pollutants present different structures and

degrees of polarity (Table 1). The elimination of these kinds of contaminants has attracted a great interest due to their difficult extraction from water because of their high affinity to water.⁶¹

The main aim of this study is to design triazole-containing poly(ether-pyridine)s as new synthetic adsorbent phases for pollutants removal in water. The obtained polymers were fully characterized using NMR spectroscopy, GPC, DSC and ATG and then their uptake performance to eliminate organic compounds was determined using High Performance Liquid Chromatography (HPLC).

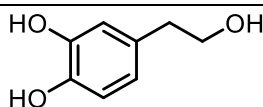
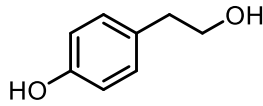
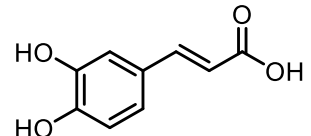
Experimental Section

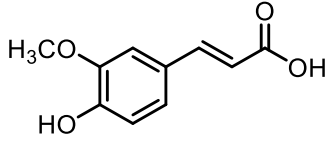
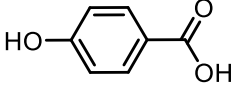
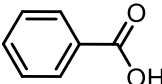
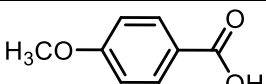
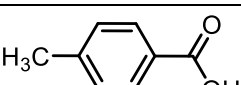
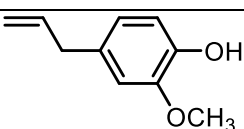
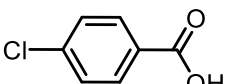
2.1. Reagents and standards

N,N-dimethylformamide (DMF, 99.9%), tetrahydrofuran (THF, 99.9%), dichloromethane (CH₂Cl₂, 99.9%), pentafluoropyridine (99%), 2,6-difluoropyridine (99%), morpholine (99%), triethylamine (99.5%), propargyl alcohol (99%), potassium carbonate (99%), sodium azide (99.5%), copper (I) bromide (98%), copper (II) acetate monohydrate (99%), sodium ascorbate (98%), 2-methyl-3-butyn-2-ol (98%) and anhydrous magnesium sulfate (99.5%) were purchased from Sigma- Aldrich and used as received. Bisphenol A (Aldrich, 99.0%) was recrystallized from toluene and isosorbide (99%) was recrystallized from acetone and dried under vacuum.

Eleven phenolic compounds (hydroxytyrosol, tyrosol, caffeic acid, ferulic acid, 4-hydroxybenzoic acid, benzoic acid, p-anisic acid, p-toluic acid, eugenol, p-chlorobenzoic acid, (E)-anethol) were selected as target pollutants for the present study because they showed markedly different physicochemical properties in terms of water solubility, molecular weight, Log *K_{ow}* and p*K_a*. All the organic pollutants were purchased from Sigma- Aldrich with a purify higher than 99%. The molecular structures of these compounds and their physicochemical properties are listed in **Table 1**.

Table 1: Structures and physicochemical properties of phenolic compounds.

Target compounds	Chemical Structure	Molecular weight (g/mol)	p <i>K_a</i> ^a	Log <i>K_{ow}</i> ^b	Water solubility (g/L)
Hydroxytyrosol		154.16	9.45	-0.7	
Tyrosol		138.16	10.12	0.04	
Caffeic acid		180.16	4.62	1.15	< 1

Ferulic acid		194.18	4.58	1.51	5.97
4-Hydroxybenzoic acid		138.12	4.5	1.58	5
Benzoic acid		122.12	4.2	1.87	3.4
P-anisic acid		152.15	4.47	1.96	0.53
P-toluic acid		136.15	4.37	2.27	0.34
Eugenol		164.20	10.19	2.49	2.46
P-chlorobenzoic acid		156.56	3.98	2.65	0.072
(E)-Anethol		148.20	-4.8	3.4	0.11

^{a)} acid dissociation constant; ^{b)} Octanol- water partition coefficient

2.2. Characterization Methods

¹H, ¹³C and ¹⁹F NMR spectra were recorded on a Bruker Advance spectrometer (300 MHz) in CDCl₃ or DMSO-*d*₆ using TMS and CFCl₃ as internal references. The MALDI-TOF mass spectra were performed on an UltraflexIII (BrukerDaltonics) mass spectrometer including a time-of-flight analyzer.

Water contact angle measurements on the polymeric film surface were obtained using a Dataphysics Digidrop contact anglemeter equipped with a CDD2/3 camera with the sessile drop method and by using Milli-Q quality water as probe liquid (volume of the drop: 2 μL). The presented results are the average of at least three measurements on different parts of each sample.

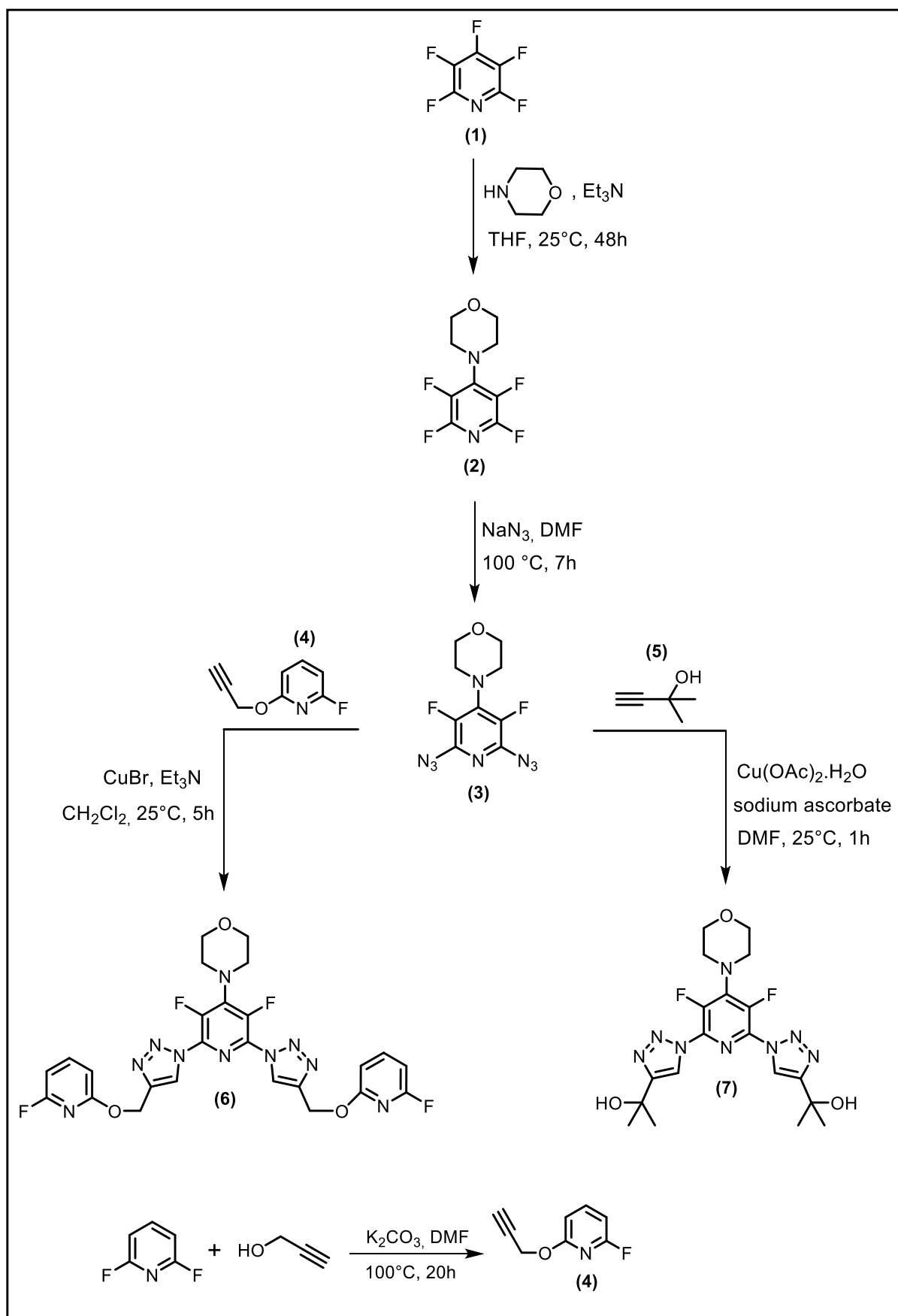
Thermogravimetric analysis (TGA) measurements were performed under nitrogen using a TGA Q50 (TA Instruments) at a heating rate of 10 °C/min from 25 to 500°C. Polymer glass transition temperatures (*T*_g) were determined by Differential Scanning Calorimetry (DSC) using a Mettler-Toledo DSC822e. DSC experiments were performed under nitrogen at a heating rate of 10°C /min from 25 to 230°C.

Molecular weights were obtained by size exclusion chromatography (SEC) using a system consisting of a pump, three PL gel-mixed columns Styragel HR0.5-HR1-HR2

(polystyrene/divinylbenzene), a refractive index (RI) detector and Shimadzu RID-10A refractometer. THF was used as the mobile phase at a flow rate of 1 mL/min. Molar masses were evaluated by means of a relative and universal method based on polystyrene standards.

2.3. Monomer Synthesis

The synthetic pathway leading to the synthesis of target fluorinated monomers (**6** and **7**) is shown in Scheme 1.



Scheme 1. Synthesis of 1,2,3-triazole-based fluorinated monomers (6-7).

2.3.1. Synthesis of 4-morpholino-2, 6, 3, 5- tetrafluoropyridine (2)

In a 500 mL three round-bottom flask equipped with a condenser and N₂ inlet, pentafluoropyridine **1** (10 g, 0.059 mol) and triethylamine (15.564 g, 0.153 mol) were dissolved in THF (160 mL). A solution of morpholine (5.227g, 0.06 mol) and THF (16 ml) was added dropwise and the mixture was then stirred 48 h at room temperature. After evaporation of the solvent (THF), 70 ml of water was added to the residue and then extracted with diethyl ether (3 × 60 mL). The organic layer was dried over MgSO₄, filtered, and concentrated under reduced pressure. The crude product was crystallized into petroleum ether, filtered, and dried under vacuum, giving a white cristal with a yield of 78%. Its chemical structure was confirmed by ¹H, ¹³C and ¹⁹F NMR (Figure S1).

¹H NMR (300 MHz, CDCl₃): δ (ppm): 3.49 (m, 4H); 3.82 (m, 4H). ¹³C NMR (75MHz, CDCl₃): δ (ppm): 50.42 (t, ⁴J_{C-F} = 4.5 Hz); 66.67 (s); 135.0, 139.76, 144.81 (3m). ¹⁹F NMR (282 MHz, CDCl₃): δ (ppm): -92.69 (s, 2F); -154.31 (s, 2F).

2.3.2. Synthesis of 4-morpholino-2,6-diazido-3,5-difluoropyridine (3)

In a 100 mL two necked round-bottomed flask, a solution of compound (2) (3 g, 12.7 mmol) and NaN₃ (3.30 g, 50.81 mmol) in 25 mL of DMF was stirred for 7 h at 100°C. After cooling, the reaction mixture was poured into water, filtered, and dried under vacuum, giving a light brown powder (71%). Its structure and purity were checked through NMR spectra (Figure S2). ¹H NMR (300 MHz, CDCl₃): δ (ppm): 3.38 (m, 4H); 3.78 (m, 4H). ¹³C NMR (75MHz, CDCl₃): δ (ppm): 50.49 (t, ⁴J_{C-F} = 4.5 Hz), 67.05 (s), 136.93 (m), 138.83 (dd, ¹J_{C-F} = 255 Hz, ³J_{C-F} = 1.5 Hz). ¹⁹F NMR (282 MHz, CDCl₃): δ (ppm): -146.02 (s, 2F).

2.3.3. Synthesis of 2-fluoro-6-(propargyloxy)pyridine (4)

Propargyl alcohol (3.165 g, 56.47 mmol) was added dropwise to a solution of 2,6-difluoropyridine (5 g, 43.44 mmol) and potassium carbonate (14.40 g, 104.25 mmol) in 30 mL of DMF. After 20 h at 100°C, the mixture was extracted with ethyl acetate (3 × 50 mL), dried with MgSO₄ and the solvent evaporated to dryness to afford the title compound (4) as yellow oil in 84% yield. This product was characterized by ¹H, ¹³C and ¹⁹F NMR analysis (Figure S3). ¹H NMR (300 MHz, CDCl₃): δ (ppm): 2.49 (t, 1H); 4.92 (d, 2H); 6.50 (dd, 1H, ³J_{H-H} = 6 Hz, ⁴J_{H-H} = 3 Hz); 6.66 (dd, 1H, ³J_{H-H} = 6 Hz, ⁴J_{H-H} = 3 Hz); 7.66 (dd, 1H, ³J_{H-H} = 9 Hz, ³J_{H-H} = 9 Hz). ¹³C NMR (75 MHz, CDCl₃): δ (ppm): 53.93 (s); 74.74 (s), 78.40 (s); 100.82 (d, ²J_{C-F} = 34.5 Hz); 107.3 (d, ⁴J_{C-F} = 4.5 Hz); 142.88 (d, ³J_{C-F} = 7.5 Hz); 161.46 (d, ³J_{C-F} = 13.5 Hz); 161.95 (d, ¹J_{C-F} = 240 Hz). ¹⁹F NMR (282 MHz, CDCl₃): δ (ppm): -70.13 (s, 1F).

2.3.4. Synthesis of monomer (6)

A mixture consisting of **3** (3 g, 10.63 mmol), **4** (3.23 g, 21.36 mmol), Et₃N (7.74g, 76.53 mmol) and CuBr (0.22 g, 1.488 mmol) in CH₂Cl₂ (30 mL) was stirred at room temperature for 5h. The reaction solution was then passed through a column of celite using 100% CH₂Cl₂ to remove residual copper (was then filtered on celite..). After evaporation of solvent, the crude product

was purified again by column chromatography on silica gel, eluting with a 8:2 mixture of petroleum ether and ethyl acetate to remove any residual starting material 3 and 4. The monomer 6 was isolated as a yellow powder (93%).

This product was characterized by ^1H , ^{13}C and ^{19}F NMR analysis (Figure S4).

^1H NMR (300 MHz, CDCl_3): δ (ppm): 3.55 (m, 4H); 3.80 (m, 4H); 5.49 (s, 4H); 6.44 (dd, 2H, $^3J_{\text{H-H}} = 6$ Hz, $^4J_{\text{H-H}} = 3$ Hz); 6.60 (dd, 2H, $^3J_{\text{H-H}} = 6$ Hz, $^4J_{\text{H-H}} = 3$ Hz); 7.60 (dd, 2H, $^3J_{\text{H-H}} = 9$ Hz, $^3J_{\text{H-H}} = 9$ Hz), 8.25 (s, 2H). ^{13}C NMR (75 MHz, CDCl_3): δ (ppm): 50.83 (t, $^4J_{\text{C-F}} = 3.75$ Hz); 59.30 (s), 67.02 (s); 100.63 (d, $^2J_{\text{C-F}} = 35.25$ Hz); 107.45 (d, $^4J_{\text{C-F}} = 5.25$ Hz); 123.77 (s); 132.67 (m); 139.29 (t, $^2J_{\text{C-F}} = 9$ Hz); 142.92 (d, $^3J_{\text{C-F}} = 7.5$ Hz); 143.45 (dd, $^1J_{\text{C-F}} = 266.25$ Hz, $^3J_{\text{C-F}} = 3.75$ Hz); 143.48 (s); 162.01 (d, $^1J_{\text{C-F}} = 240$ Hz); 162.04 (d, $^3J_{\text{C-F}} = 13.5$ Hz). ^{19}F NMR (282 MHz, CDCl_3): δ (ppm): -70.21 (s, 2F); -133.76 (s, 2F).

2.3.5. Synthesis of monomer (7)

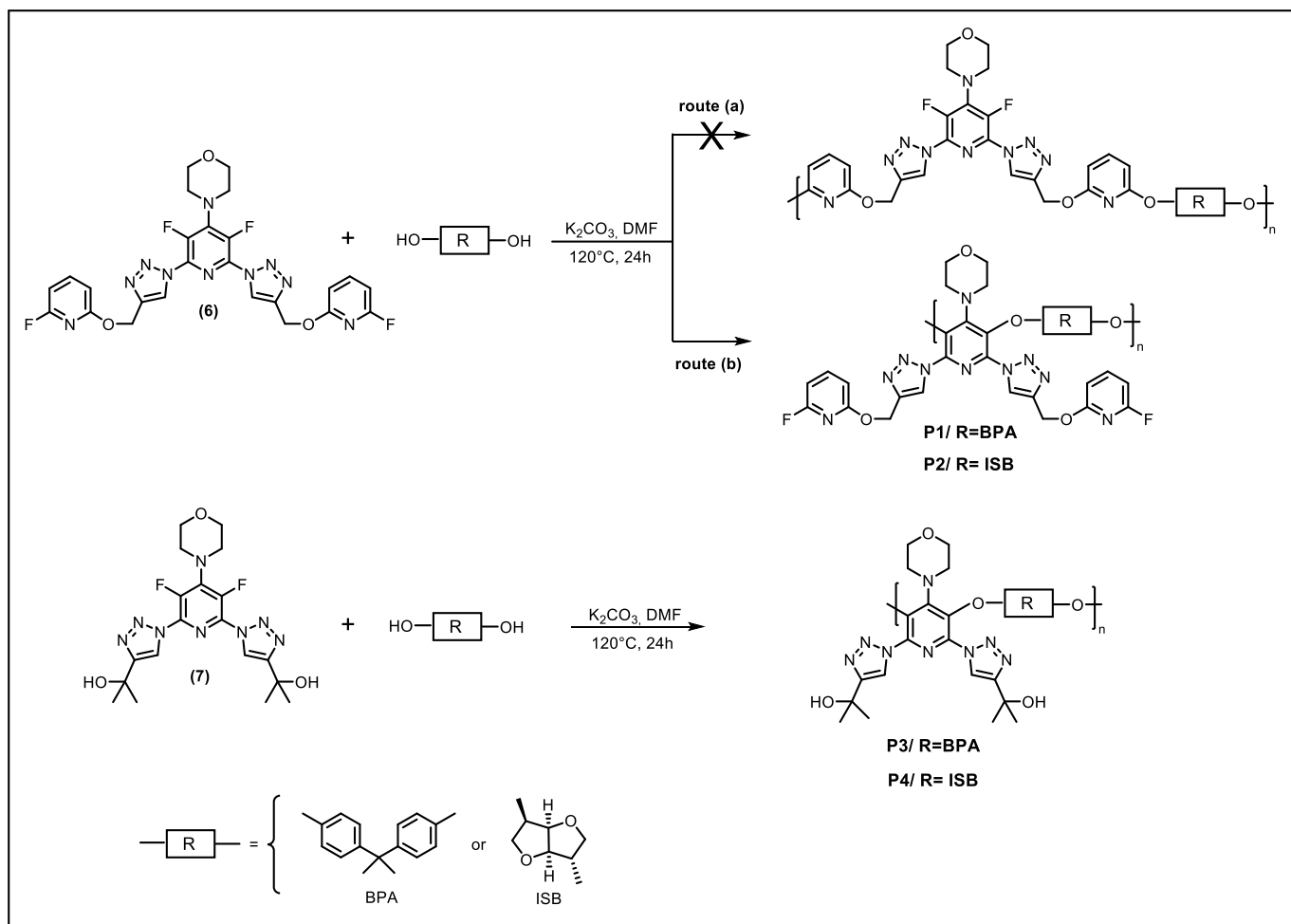
2 g (7.08 mmol) of 3, 1.198 g (14.24 mmol) of 2-methyl-3-butyn-2-ol, $\text{Cu}(\text{OAc})_2 \cdot \text{H}_2\text{O}$ (20 mol%), and sodium ascorbate (40 mol%) were mixed in DMF (12 mL) at room temperature for 1h. The mixture was extracted with dichloromethane (3×30 mL), dried over MgSO_4 , and concentrated by rotary evaporation. The crude product was further purified by column chromatography on silica gel with 100% ethyl acetate as eluent to afford the corresponding pure monomer 7 as white powder with a yield of 80 %.

This product was characterized by ^1H , ^{13}C and ^{19}F NMR analysis (Figure S5).

^1H NMR (300 MHz, CDCl_3): δ (ppm): 1.63 (s, 12H); 2.88 (s, 2H); 3.54 (m, 4H); 3.79 (m, 4H); 8.04 (s, 2H). ^{13}C NMR (75 MHz, CDCl_3): δ (ppm): 30.36 (s); 50.80 (t, $^4J_{\text{C-F}} = 4.5$ Hz); 67.03 (s, Cb); 68.59 (s, Ch); 119.57 (s); 132.69 (m); 139.20 (t, $^2J_{\text{C-F}} = 9$ Hz); 143.3 (dd, $^1J_{\text{C-F}} = 266.25$ Hz, $^3J_{\text{C-F}} = 3.75$ Hz); 155.56 (s). ^{19}F NMR (282 MHz, CDCl_3): δ (ppm): -134.06 (s, 2F).

2.4. Polymer synthesis

The following general procedure, as illustrated in Scheme 2, was used for the preparation of all PEPTs (P1- P4). In a two-necked reactor equipped with a N_2 inlet and a mechanical stirrer, a mixture of 0.8559 mmol isosorbide or bisphenol A, 0.8559 mmol (6) or (7), 1.883 mmol K_2CO_3 and 3 mL of DMF (20% solid) was stirred and heated at 120°C for 24 h. The solution was then poured into a large volume of water. The precipitate was collected by filtration, washed thoroughly with water and dried in a vacuum oven at 80°C for 24 h. The yields of the polymerization reactions were in the range of 78–96 %.



2.5. Adsorption studies

2.5.1. Preparation of doped solution

Preparation of polyphenols solution MC1

Solution of target molecules MC1 were prepared by dissolving a defined weight of phenolic compounds in 1 L of distilled water in order to obtain an equal molar concentration (25 μ mol/L). 2 mL of orthophosphoric acid was then added to adjust the pH solution to 2. The mixture was stirred over a night until the total dissolution of the pollutants.

2.5.2. Chromatographic analysis and conditions

The adsorption of phenolic compounds was performed by High Performance Liquid Chromatography (HPLC) equipped with an Agilent XDB C18 column (3 mm x 100 mm x 1.8 μ m) at an oven temperature of 40 $^{\circ}$ C. The diode array detector was set at the wavelength of 210 nm. The elution rate of mobile phase, which consisted of 0.1% (vol/vol) of orthophosphoric acid in water (eluent A) and acetonitrile (eluent B), was fixed at 1 mL/ min. The injection volume of samples was adjusted at 5 μ L. The amount of target molecules adsorbed by the

polymer was determined by the difference between areas of chromatographic peaks, before and after extraction.

The retention times of: Hydroxytyrosol, Tyrosol, P-hydroxybenzoic acid, Caffeic acid, Ferulic acid, Benzoic acid, P-anisic acid, P-toluic acid, P-chlorobenzoic acid, Eugenol, and (E)-Anethol under the above HPLC conditions were: 2.2-2.5, 3.8-4.2, 5.5-6.0, 6.7-7.2, 9.0-9.5, 10.0-10.5, 10.7-11.2, 12.3-12.8, 12.8-13.3, 13.5-14.0, and 15.8-16.3 minutes, respectively.

2.5.3. Adsorption experiments

Adsorption tests of polymers toward polyphenols were performed by batch technique, in 20 mL scintillation flasks, 60 mg of polymers (adsorbents), 3 g of sodium chloride (NaCl) and 10 mL of pollutants solution (MC1) were mixed with magnetic stir bars (900 tr/min) at room temperature. At predetermined sampling times (1, 3, 5, and 24 hours), 0.5 mL of samples were collected via a 2.5 mL syringe and filtered through a 0.45 μm PTFE filter into vial. The vials were then transferred for HPLC analysis.

The efficiency of pollutants removal (in %) by the sorbent phase was calculated by the following equation

$$\text{Pollutant removal efficiency} = (\text{Ac}_{\text{Mix}} - \text{Ac}_{\text{T}} / \text{Ac}_{\text{Mix}}) \times 100$$

Where Ac_{Mix} and Ac_{T} are the areas of chromatographic peak of organic pollutants in the original solution and the filtrate after extraction, respectively.

1. Results and discussion

1.1. Synthesis and characterization of monomers

New fluorinated monomers containing 1,2,3-triazole units (**6**, **7**) were successfully prepared in three steps from pentafluoropyridine (**1**). The first step of the strategy, outlined in Scheme 1, requires the synthesis of 4-substituted tetrafluoropyridine via nucleophilic aromatic substitution of pentafluoropyridine (**1**) with morpholine. The reaction was carried out in the presence of Et_3N in THF, as reported in the literature^{51,62}, giving a white crystal of 4-morpholino-tetrafluoropyridine (**2**) in 78% yield. Upon treatment of 4-morpholino-tetrafluoropyridine (**2**) with an excess (molar ratio 1:4) of sodium azide in DMF at 100 °C for 7h afforded 4-morpholino-2,6-diazido-3,5-difluoropyridine (**3**) in modest isolated yield (71%). The regioselectivity of the various nucleophilic substitution reactions of pentafluoropyridine was established by ^{19}F NMR studies.

The ^{19}F NMR spectrum, illustrated in Figure 1, shows the sequential conversion of pentafluoropyridine (**1**) to intermediate (**2**) and to compound (**3**). The spectrum of (**1**) shows three chemically shifted peaks at -86.39 ppm (ortho-F, F1), -132.38 ppm (para-F, F3) and -162.52 ppm (meta-F, F2) with a relative integration ratio of 2:1:2. In the ^{19}F NMR spectra of (**2**), two peaks for fluorines are observed at -92.69 and -154.31 ppm attributed to ortho and meta fluorine atoms, respectively, while the signal assigned to fluorine atom located at the 4-position of pentafluoropyridine (F3) has disappeared. These results confirm that the nucleophilic substitution of fluorine occurs, as expected, at the para-position to ring nitrogen due to the strong -I effect of N-atom^{63, 64}. Only one signal related to meta fluorine atoms (F2) is

appearing in the ^{19}F NMR spectra of diazide (**3**) at -146.02 ppm, which indicates that the two azide groups in the molecule are located in ortho position of the pyridine ring.

The 2-fluoro-6-(propargyloxy)pyridine (**4**), used for the preparation of monomer (**6**), was obtained by nucleophilic substitution of 2,6-difluoropyridine with propargyl alcohol in the presence of potassium carbonate in DMF yielding (**4**) as yellow oil in 84% yield. Finally, the 1,2,3-triazole-based fluorinated monomers (**6** and **7**), were synthesized by Cu(I)-catalyzed 1,3-dipolar cycloaddition reaction (CuAAC) with calculated stoichiometric molar ratios 1:2 of diazide (**3**) and propargyl compounds (**4**) or (**5**) for **6** and **7** synthesis, respectively. The CuAAC reaction of (**3**) with (**4**) was catalyzed by CuBr (0.14 equiv) and triethylamine (7.2 equiv) according to azide or alkyne functionalities in CH_2Cl_2 at room temperature. Following a previously described procedure⁶⁵, the synthesis of monomer (**7**) was carried out in the presence of 20% of $\text{Cu}(\text{OAc})_2 \cdot \text{H}_2\text{O}$ and 40% of sodium ascorbate as the catalyst in DMF for 1h at room temperature. In the synthesis progress of (**6**) the solution was colorless, after the catalyst was added the color became green 10 min later then turned to black after 1h, and the reaction released heat during the process. The yields of (**6**) and (**7**) were 93% and 80%, respectively.

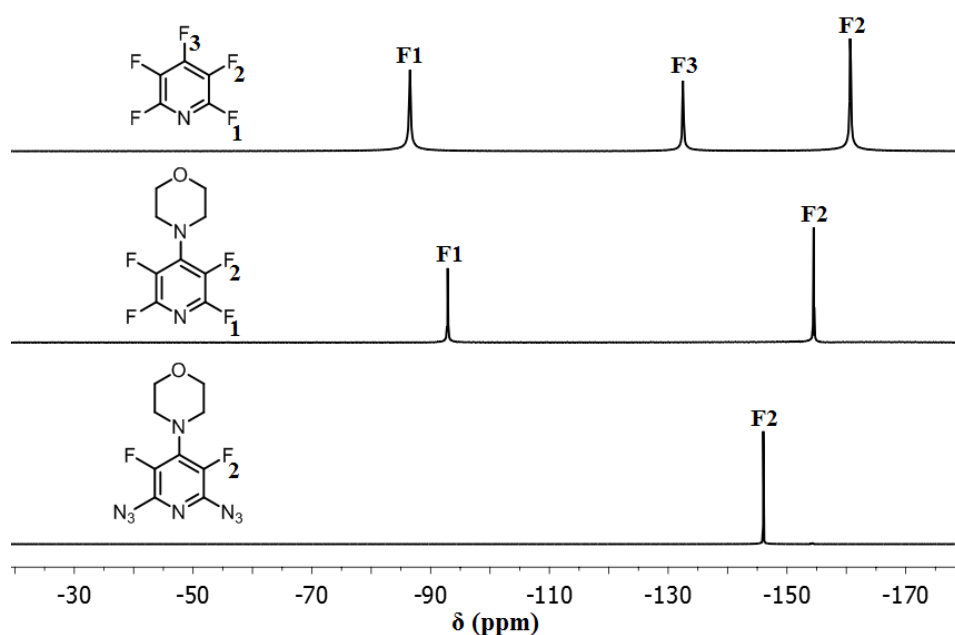


Figure 1. ^{19}F NMR spectra of PFP (**1**), (**2**) and (**3**) in CDCl_3 .

The obtained 1,2,3-triazole-based monomers (**6** and **7**) were characterized by ^1H , ^{13}C and ^{19}F NMR given in the experimental sections. The cycloaddition reactions between diazide and alkyne compounds were confirmed by the appearance of the characteristic signal of triazole rings in ^1H NMR spectra at 8.25 for monomer (**6**) and 8.04 ppm for monomer (**7**) as well as the disappearance of the alkyne signals (Figures S4 and S5 in Supporting Information).

1.2. Synthesis and characterization of polymers

The obtained monomers were employed to synthesize a series of novel poly(ether-pyridine)s bearing 1,2,3-triazole moieties as pendent chains (P1-P4) by polycondensation with two diols:

isosorbide and bisphenol A (Scheme 2). The polymerization of equimolar amounts of monomers was performed in the presence of potassium carbonate in DMF at 120°C. The polymers were isolated in different yields (78-96 %) after precipitation in water and dried under vacuum. The chemical structures of the synthesized polymers were confirmed by ¹H, ¹⁹F NMR and MALDI-TOF mass spectrometry.

The structural composition of the resulting monomer (6)-based polymers (P1 and P2) was determined using MALDI-TOF mass spectrometry by comparison between the calculated and measured peak intensities related to each of the possible produced structures La, Lb, Lc, and C as shown in Figures 3A and 4A. The corresponding calculated masses of each of the formed structures illustrated in Figures 3A and 4A are summarized respectively in Table 2 and 3.

The mass spectrum of P1 issued from condensation of BPA and fluorinated monomer (6) (Figure 3B) clearly showed the presence of only one series of peaks with a repeating unit 772.77 Da attributed to potassium-cationized cyclic structures C. These results prove the total conversion of monomers. The obtained structures C could be resulted from the condensation of OH functional groups of BPA with ortho-fluorine (structures C') or meta-fluorine atoms of monomer (6) (structures C'') followed by a cyclization reaction. In fact, there are two possibilities which F-atoms of monomer (6) can react. On the one hand, the ortho F-atoms to the N of difluoropyridine (F1) can react with the diol via S_{Ar}N (Scheme 2, route a) or on the other hand the F atoms in meta-position to the N of pentafluoropyridine (F2) react with diol (Scheme 2, route b).

In order to investigate which of the F-atoms of monomer (6) were displaced by OH-diols, since the reactivities of F-atoms in this monomer for nucleophilic displacement reactions are different, the polymer P1 was characterized with ¹⁹F NMR. The ¹⁹F NMR spectra of polymer P1 (Figure 2) shows one peak at -70.14 ppm attributed to (ortho) fluorine atoms (F1) by comparing the spectra of monomer and the signal at -133.76 ppm related to (meta) fluorine atoms (F2) of monomer has disappeared after polymerization. The obtained results illustrate that the condensation of monomer (6) with bisphenol A (or isosorbide) proceeds regioselectively at the meta position to afford the corresponding PEPT P1 (Scheme 2), contrary to the results previously obtained by Gomri et al⁵¹. They reported that the polycondensation of pyridinium fluorinated monomers with diols was performed in the positions 2 and 6 of pentafluoropyridine and the fluorine atoms in meta positions were not activated even at a high temperature. The regioselectivity of nucleophilic addition in our process can be explained by the high electron-withdrawing effect of triazole units that activate the meta site toward diol attack. Based on the polymerization results of monomer (6), we are interested in our study to synthesize a second 1,2,3- triazole based- monomer (7) containing hydroxyl groups in order to increase the hydrophilicity of the resulting PEPTs (P3 and P4) which contributed to the enhanced adsorption capacity of these polymers.

The ¹H NMR spectrum of polymer P1 presented in Figure S6 exhibited the characteristic protons of BPA (Hh–Hj) and of the monomer (6) (Ha–Hg). The absence of end-groups on the NMR spectra confirmed the high-molecular weight of the resulting polymer (96%), as well as the formation of cyclic structures C.

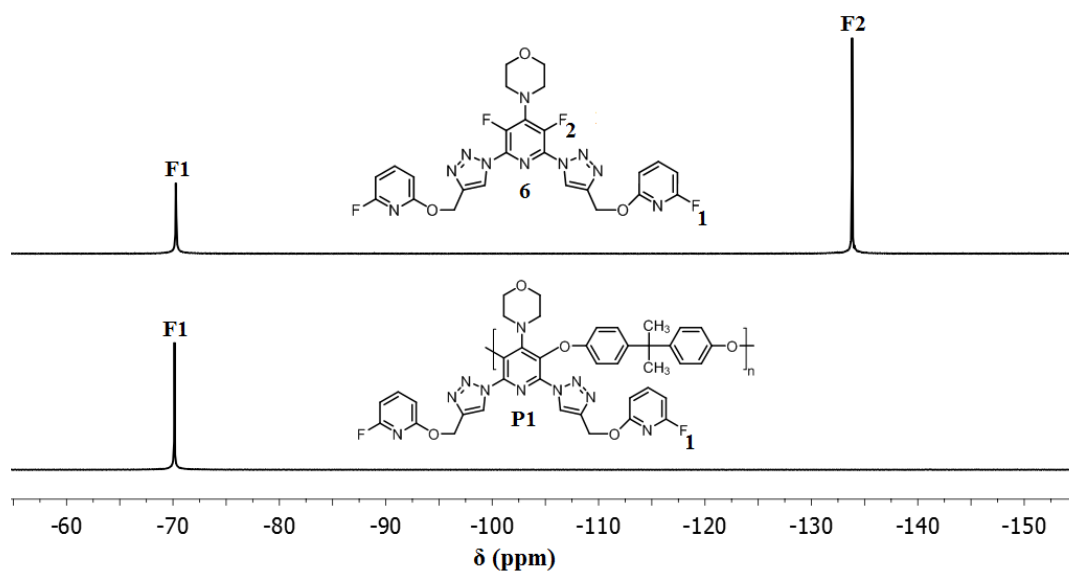
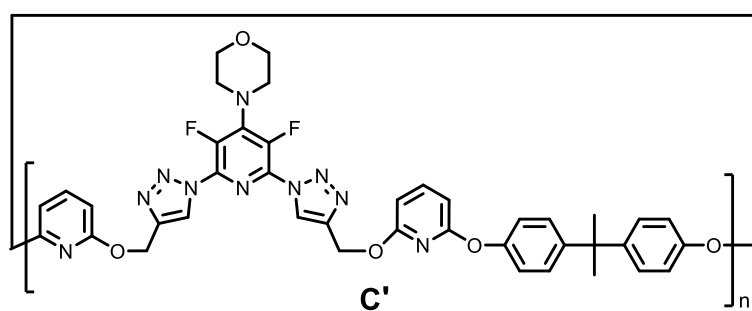
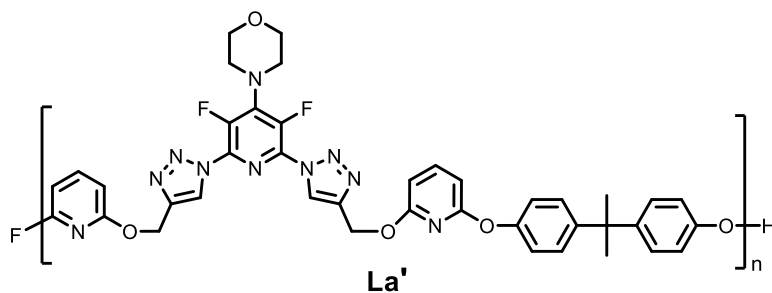


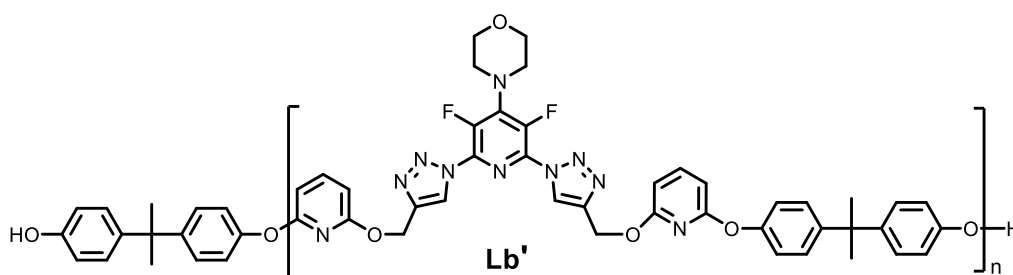
Figure 2. ^{19}F NMR spectrum of monomer (6) and PEPT (P1).



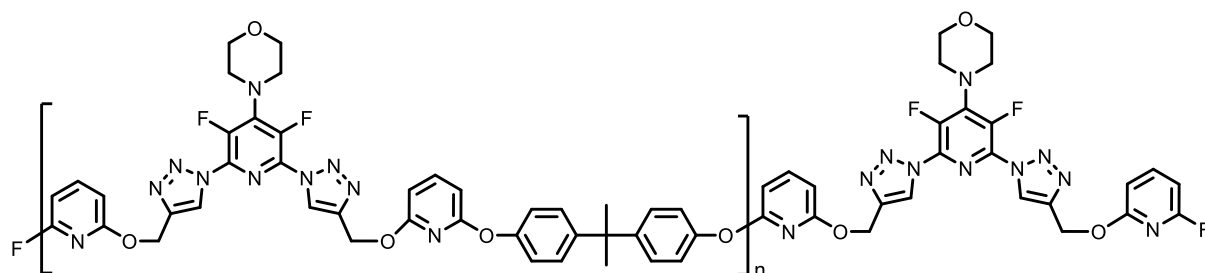
$$M_{th} = (772.77 * n) \text{ g.mol}^{-1}$$



$$M_{th} = (772.77 * n + 20.01) \text{ g.mol}^{-1}$$



$$M_{th} = (772.77 * n + 228.29) \text{ g.mol}^{-1}$$



$$M_{th} = (772.77 * n + 584.50) \text{ g.mol}^{-1}$$

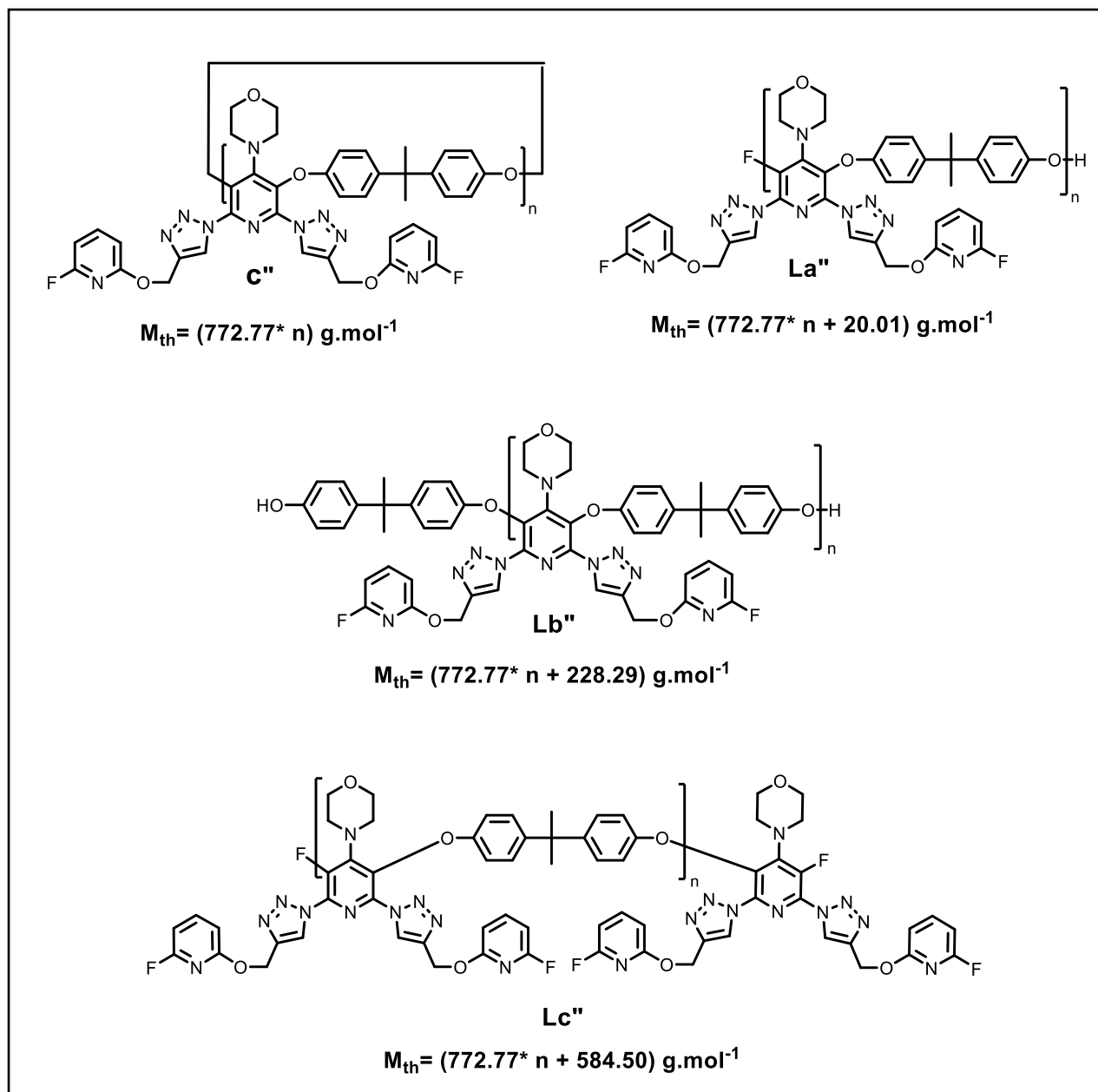


Figure 3A. Possible reaction products of P1 obtained after polycondensation of monomer (6) with BPA.

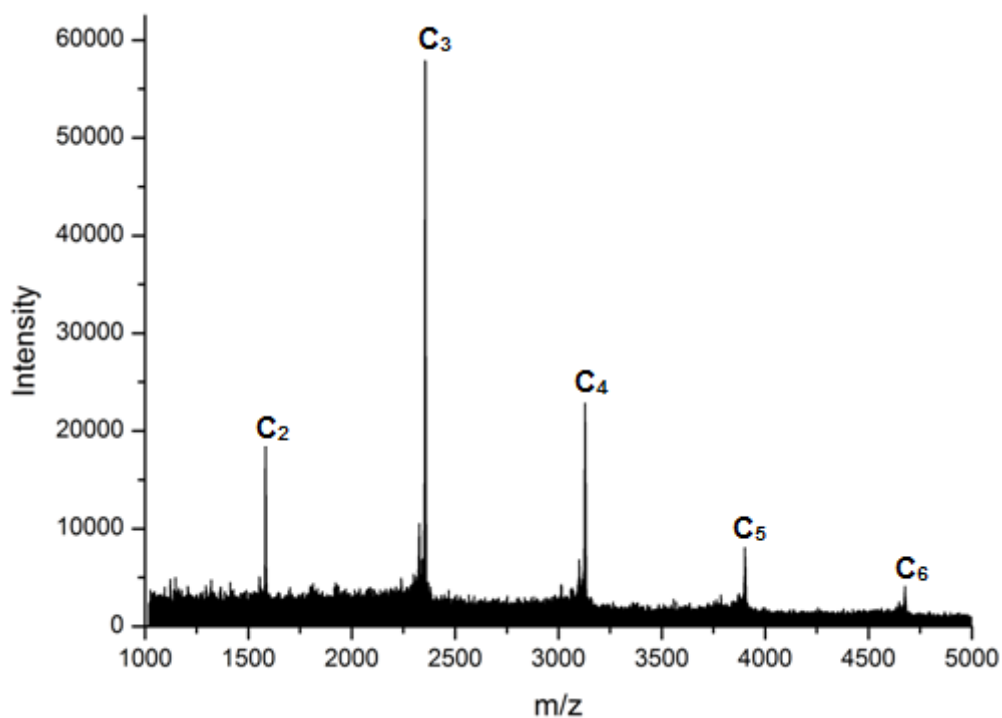


Figure 3B. MALDI-TOF mass spectrum of P1.

Table 2. Calculated masses (including K_doping) of the potential reaction products C, La, Lb and Lc (P1).

DP	C	La	Lb	Lc
2	1584.6	1604.6	1812.9	2169.1
3	2357.4	2377.4	2585.7	2941.9
4	3130.2	3150.2	3358.5	3714.7
5	3902.9	3923.0	4131.2	4487.4
6	4675.7	4695.7	4904.0	5260.2
7	5448.5	5468.5	5676.8	6033.0

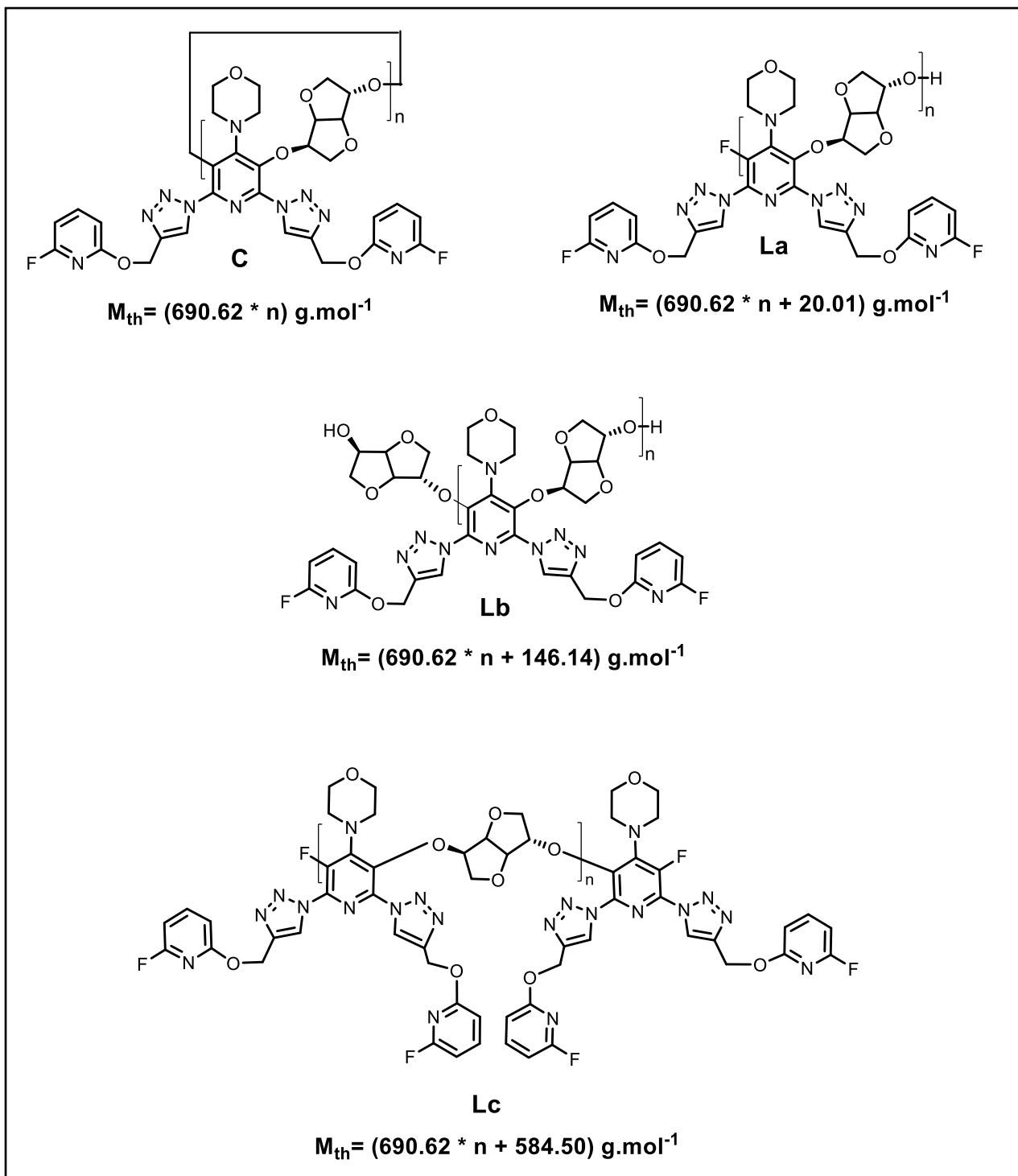


Figure 4A. Possible reaction products of P2 obtained after polycondensation of monomer (6) with ISB.

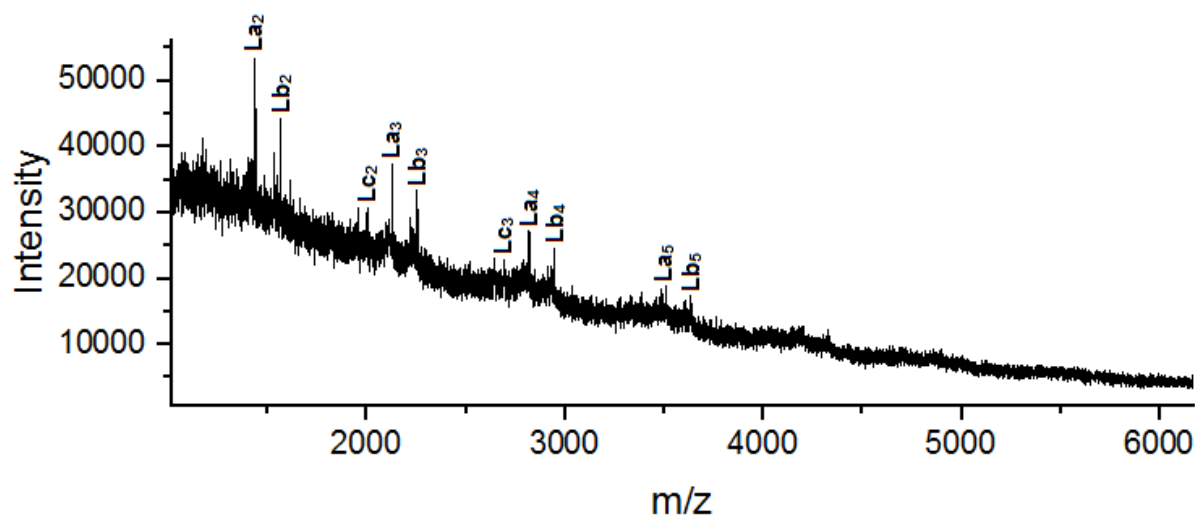


Figure 4B. MALDI-TOF mass spectrum of P2.

Table 3. Calculated masses (including K₂ doping) of the potential reaction products C, La, Lb and Lc (P2).

DP	C	La	Lb	Lc
2	1420.3	1440.3	1566.5	2004.8
3	2111.0	2131.0	2257.1	2695.5
4	2801.6	2821.6	2947.7	3386.1
5	3492.2	3512.2	3638.3	4076.7
6	4182.8	4202.8	4329.0	4767.3

The MALDI-TOF mass spectrum of produced PEPT P2 given in Figure 4B revealed the formation of three linear chains La, Lb, and Lc that differ by the nature of end groups (Figure 4A, Table 3). The NMR analysis confirmed the interpretation obtained by MALDI-TOF analysis. We find in the ¹H NMR spectra all the characteristic protons of the repeat unit (Ha–Hm). Moreover, end-group signals (Hi*, Hl*) and (Ha*, Hb*, Hc*, Hd*) which characterized La, Lb, and Lc terminals are detectable (Figure S7). The ¹⁹F NMR spectrum presented only one signal at -70.25 ppm attributed to the fluorine F1 (Figure S7).

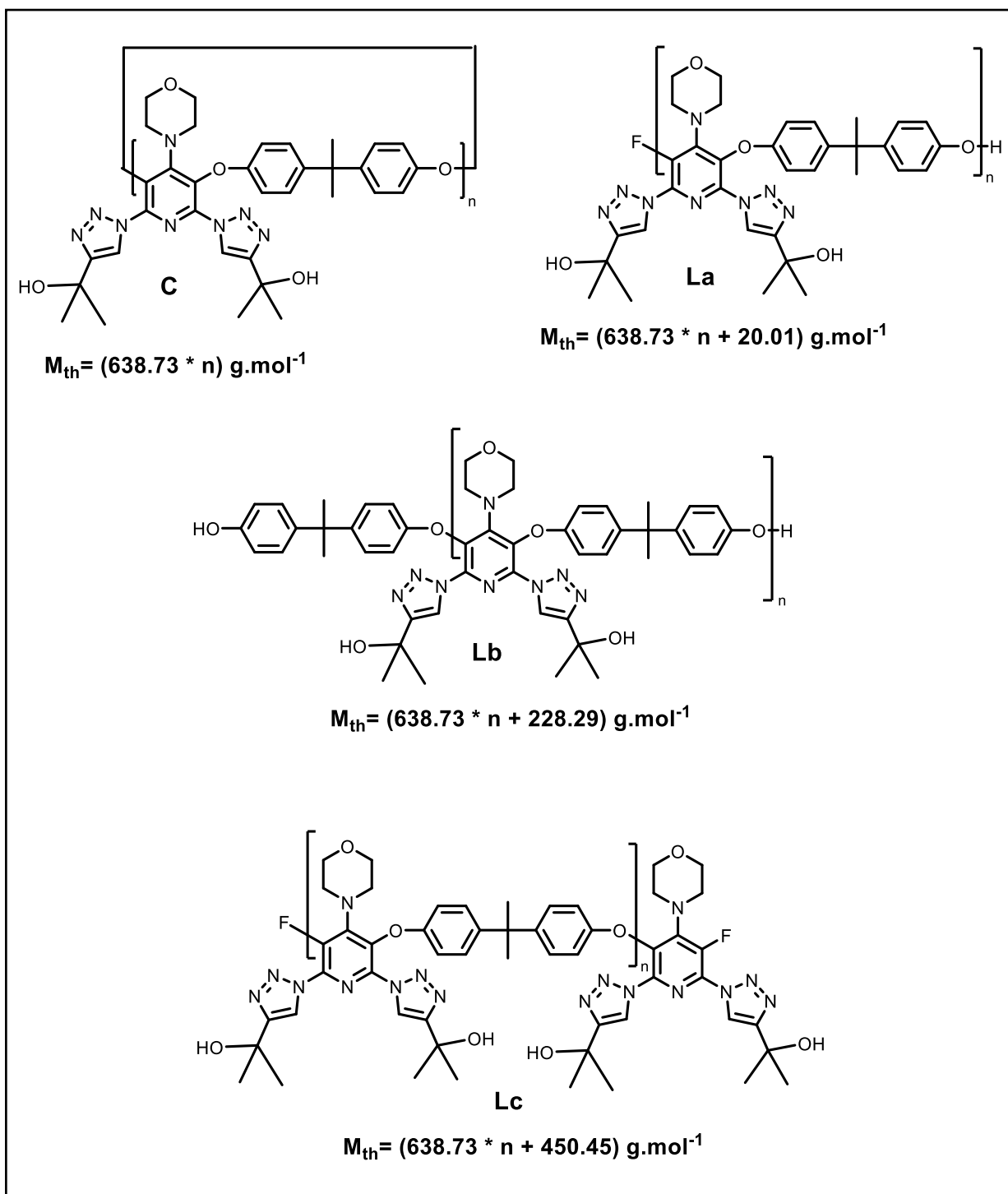


Figure 5A. Possible reaction products of P3 obtained after polycondensation of monomer (7) with BPA.

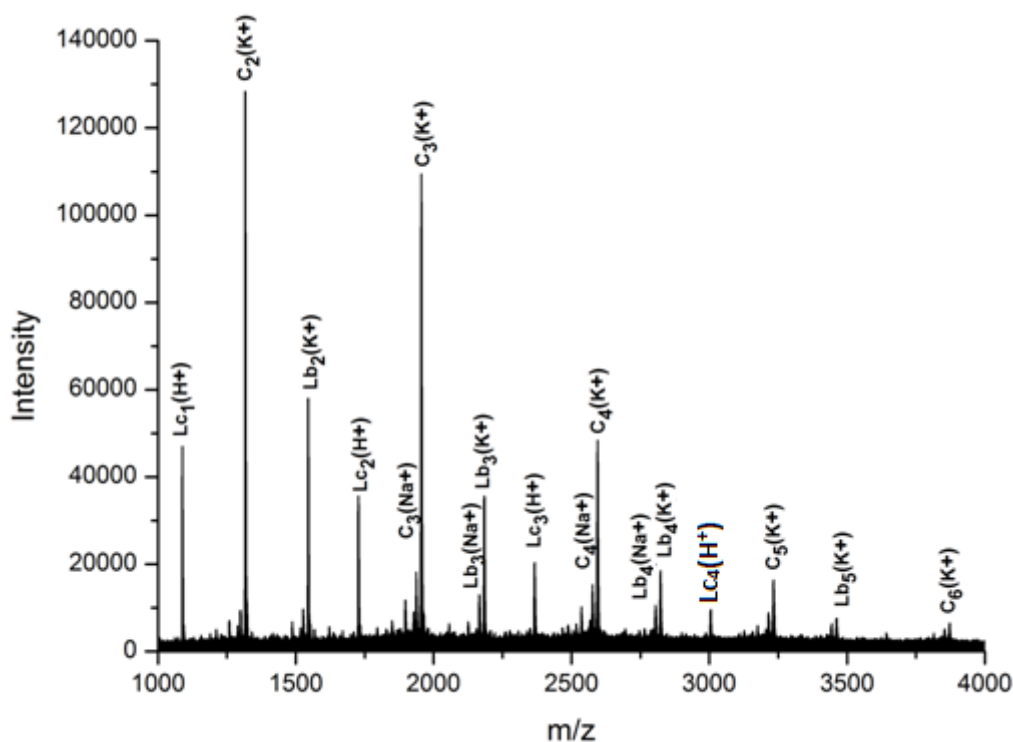


Figure 5B. MALDI-TOF mass spectrum of P3.

Table 4. Calculated masses (including K₋ doping) of the potential reaction products C, La, Lb and Lc (P3).

DP	C	La	Lb	Lc
2	1316.6	1336.6	1544.8	1767.0
3	1955.3	1975.3	2183.6	2405.7
4	2594.0	2614.0	2822.3	3044.5
5	3232.7	3252.8	3461.0	3683.2
6	3871.5	3891.5	4099.8	4321.9
7	4510.2	4530.2	4738.5	4960.7

The examination of structural composition of PEPT P3 derived from the second fluorinated monomer (7) and BPA by MALDI-TOF spectra (Figure 5B), reveals the presence of three main series of peaks with repeating unit 638.73 Da attributed to the cyclic structures C and the linear structures Lb and Lc (Figure 5A, Table 4). The presence of functional OH and F end groups indicated the incomplete conversion of monomers which justified the low molecular weight ($M_n = 4849 \text{ g.mol}^{-1}$) of polymer P3. This result was in agreement with the ^1H NMR spectra (Figure S8), which indicated the total protons characteristic of the repetitive unit with the presence of low intensity peaks corresponding to protons on the end groups of bisphenol A (Hg*et Hf*) and difluoro monomer 7 (Ha*, Hb*, Hc*, Hd*).

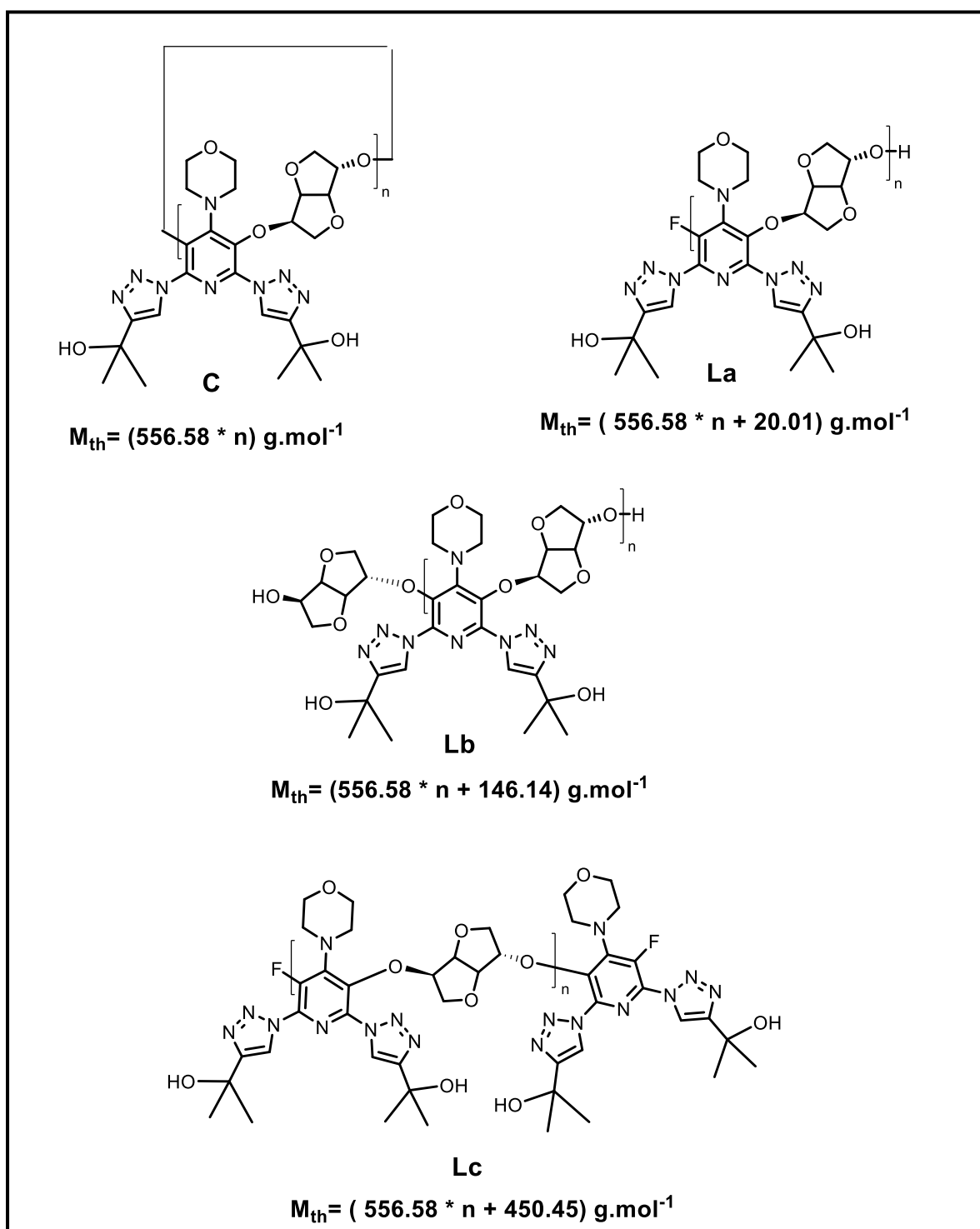


Figure 6A. Possible reaction products of P4 obtained after polycondensation of monomer (7) with ISB.

Table 5. Calculated masses (including K_doping) of the potential reaction products C, La, Lb and Lc (P4).

DP	C	La	Lb	Lc
2	1152.3	1172.3	1298.4	1602.7
3	1708.8	1728.8	1855.0	2159.3
4	2265.4	2285.4	2411.6	2715.9
5	2822.0	2842.0	2968.1	3272.4
6	3378.6	3398.6	3524.7	3829.0

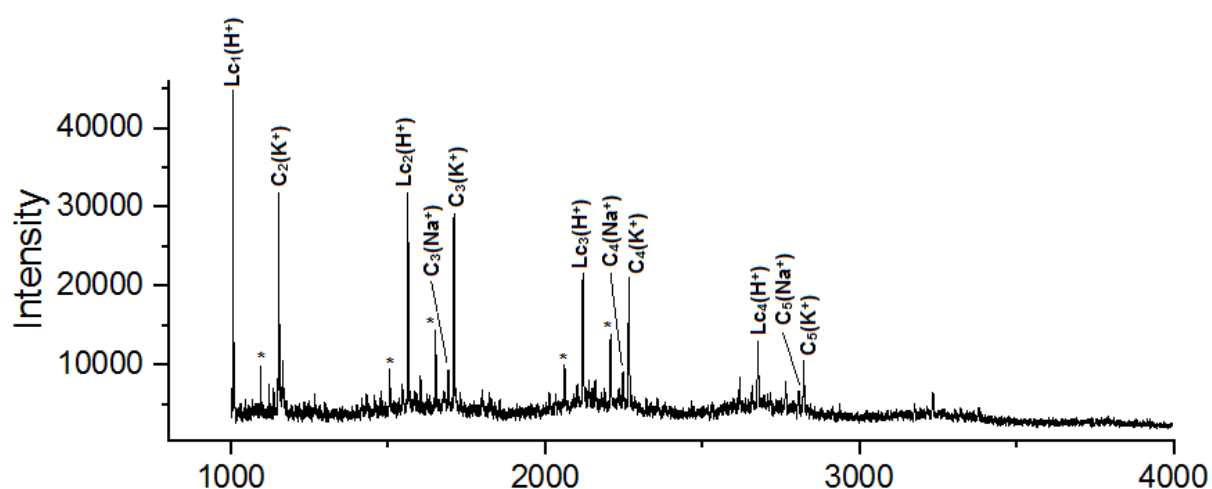


Figure 6B. MALDI-TOF mass spectrum of P4.

The MALDI-TOF mass spectra of P4 (Figure 6B) displays two series of peaks separated by 556.58 Da attributed to cyclic structures (C) and difluoro linear structures (Lc). The linear Lc structure was evidenced by signals corresponding to protons Hc* and Hd* related to fluorinated monomer (7). Furthermore, the doublet located at 5.26 ppm in the ^1H NMR spectrum (Figure S9) attributed to proton (He) related to hydroxyl group of difluoro monomer (7) can be explained by the endo and exo effect of isosorbide hydroxyl group.

Solubility of these PEPTs was tested by dissolving 10 mg of polymers in 1 ml of solvent; if there are insoluble we tested 1 mg of polymer in 1 mL of solvent. The results are summarized in Table 6.

Table 6. Solubility of PEPTs.

N°	Solvents ^[a]											
	$n\text{C}_7\text{H}_{16}$	MeOH	EtOAc	Et ₂ O	Acetone	THF	CH ₂ Cl ₂	CHCl ₃	CH ₃ CN	DMSO	NMP	H ₂ O
P1	-	-	-	-	-	++	++	++	++	++	++	-
P2	-	-	-	-	~	++	++	++	++	++	++	-

P3	-	++	-	-	~	++	~	~	-	++	++	-
P4	-	++	-	-	-	++	-	-	-	++	++	-

(++) soluble at 10 mg/mL ; (~) partially soluble at 1 mg/mL; (-) totally insoluble at 1 mg/mL

The obtained PEPTs (P1- P4) exhibited excellent solubility in aprotic polar solvents such as DMSO, DMF and NMP and in less polar solvent like THF. They are insoluble at 1 mg/mL in hexane, ethyl acetate, diethyl ether and water. The monomer (7) based-PEPTs (P3, P4) are soluble in methanol compared to monomer (6) based- PEPTs (P1, P2). The methanol as protic polar solvent very strongly solvate the polymers P3 and P4 thanks to hydrogen bonds formed between hydroxyl groups in the polymers and methanol.

The surface hydrophilicity of the polymers was assessed by contact angle measurements. The contact angle and thus the hydrophilicity of the polymers decrease in the following order: P1>P2>P3>P4 (Figure 7). These results are in good agreement with the observed solubility of P3 and P4 in methanol (Table 6). Among the poly(ether-pyridine)s series of polymers, P4 is the most hydrophilic while P1 is the more hydrophobic. Replacing the pyridinic fluoro group and bisphenol A in the polymeric phases P1, with hydroxyl groups as pendant chains and isosorbide in main chain, enhances the hydrophilicity. The wettability of the sorbent phase P4 is highly improved by the insertion of the bio-based monomer, isosorbide, and the polar hydroxyl groups will then improve the adsorption of more polar organic compounds.

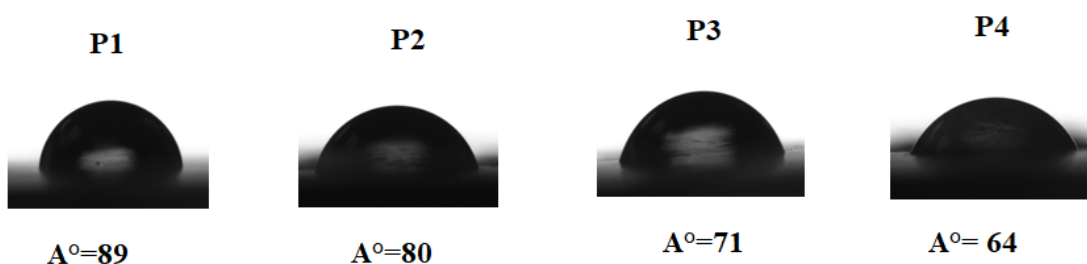


Figure 7. Contact angles of a water droplet on the polymer substrates: P1-P4

Table 7. Polymerization results and thermal properties of the resulting polymers P1-P4.

Polymer	Monomers	Yield ^{a)} (%)	T_g ^{b)} (°C)	T_{d5} ^{c)} (°C)	T_{d25} ^{d)} (°C)	M_n ^{e)} (g/mol)	M_w ^{e)} (g/mol)	PD ^{e)}
P1	6/ BPA	96	144	238	389	22372	66862	2.99
P2	6/ Is	92	146	234	313	16171	17602	1.09
P3	7/ BPA	85	178	234	315	4849	6693	1.38
P4	7/ Is	78	187 ^{d)}	239	290	3735	4910	1.32

^{a)} After precipitation into water. ^{b)} Determined by DSC under nitrogen at a heating rate of 10°C/min.

^{c)} Temperature at 5 wt % loss. ^{d)} Temperature at 25 wt % loss. ^{e)} Number and weight-averaged molecular weights and polydispersity (PD) determined by GPC in THF (calibrated with polystyrene). ^{f)} Determined by Thermomechanical analysis (TMA).

Solubility of PEPTs P1–P4 in THF allowed their characterization by SEC using THF as eluent and calibrated with polystyrene standards. The molecular weight (M_n) values of the obtained polymers are ranging from 3735 and 22372 Da and the dispersity index (PD) is between 1.3 and 2.9 (Table 7). The polymer based on monomer (6) and BPA (**P1**) exhibit the highest molecular weight ($M_n = 22372$ Da) due to the high reactivity of BPA compared to isosorbide. We can also observe that polymers based on monomer (6) (P1 and P2) showed M_n values much higher than those obtained from monomer (7) (P3 and P4). P3 and P4 can be considered as oligomers since their M_n values (4849 and 3735 Da) are in the range of 1000-5000 Da.

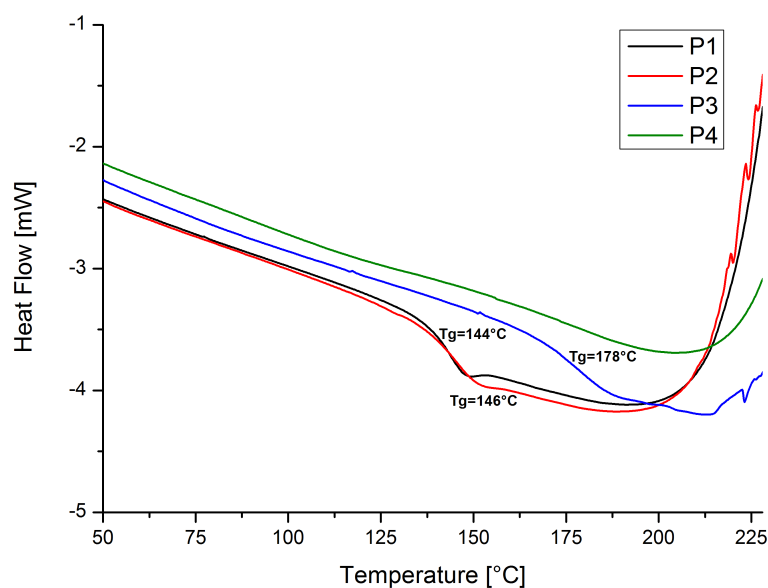


Figure 8. DSC curves of polymers P1-P4.

3.3. Thermal properties of polymers

The thermal properties of PEPTs were studied by thermogravimetric analyses (TGA) and differential scanning calorimetric (DSC). DSC experiments clearly demonstrated the amorphous behavior of poly(ether-pyridine-triazole)s with the presence of a single transition corresponding to their glass transition temperature (T_g) (Figure 8). The high T_g values ranging from 144 to 180°C (Table 7) for these polymers, depending on the structure of the diol and fluorinated components in chains. The bio-based PEPTs (P2 and P4) exhibit higher T_g compared to those of the petro-based polymers (P1 and P3), as previous work revealed^{66,67,51}, because of the high rigidity promoted by the combined presence of 1,2,3-triazole and dianhydrohexitol heterocyclic moieties. The T_g values of PEPTs derived from monomer (7) (P3, 178°C) are higher than those of PEPTs based on monomer (6) (P1, 144°C) due to the presence of inter and intra-chains hydrogen bonding between hydroxyl groups that can decrease the flexibility of the polymer chains with increasing in their T_g .

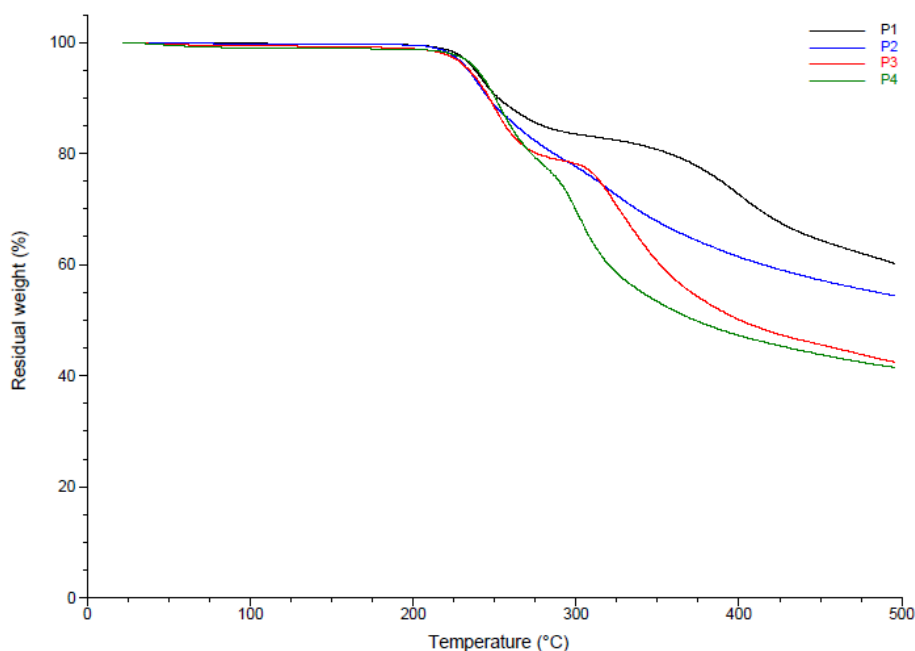


Figure 9. TGA traces of polymers P1-P4.

The TGA analyses (Figure 9 and Table 7) showed that all poly(ether-pyridine triazole)s P1-P4 were thermally stable with the decomposition temperatures for 5% weight losses (T_{d5}) at $\sim 236^\circ\text{C}$, which could be attributed to thermal decomposition of the triazole pendant groups of poly(ether-pyridine)s. Then, the main chain of the polymers started to break and decompose by the elevation of the temperature to $>300^\circ\text{C}$ depending on the structure of the polymers. The temperatures at 25% weight losses are in the range of $290\text{--}389^\circ\text{C}$. The BPA-based polymers (P1, P3) display better thermal stabilities than polymers on isosorbide (P2, P4).

3.4. Adsorption behavior of the polymers

Phenolic compounds constitute an important class of water pollutants that should be removed from wastewater due to their high toxicity for plant and aquatic organisms.

They are discharged in the liquid effluents from various factories: chemical, petrochemical, paper, wood, metallurgy and cocking plants. They are also found in the waste waters of agroindustrial processes like the olive oil mills, tomato processing and wine distilleries. Amongst the phenols that have been detected in olive oil mill waste waters (OMW)s are: hydroxytyrosol, tyrosol, caffeic acid, ferulic acid, and 4-hydroxybenzoic acid, which are among our target molecules. The aim of this study is to evaluate the adsorption efficiency of phenolic compounds on the candidate polymer adsorbents P1-P4. The influence of the hydrophobicity/hydrophilicity of pollutants and of the different chemical structures of polymers on adsorption process is also studied.

The chemical characteristics of phenolic compounds described in Table 1 ultimately determine their treatability and adsorption by polymeric phases. These compounds have an aromatic ring (benzene) and hydroxyl groups in their chemical structure and present different molecular weights. The pK_a of phenolic compounds shows the acid dissociation constant of the compound. The phenols that present a carboxylic hydroxyl (OH) group all dissociate in the

same pH range between 3.98 and 4.62. Therefore, at neutral pH ($\text{pH} > \text{pKa}$) these compounds are mainly in the form of negatively charged phenoxy ions. In order to maintain the neutral state (uncharged) of benzene derivatives compounds in water, the pH of the working solution is adjusted at 2 using orthophosphoric acid. Log K_{ow} parameter measures the hydrophobicity of the target pollutants by repartitioning between octanol and water. As a general rule, compounds with Log $K_{ow} > 2.5$ are considered as hydrophobic as low-polar compounds, and they are expected to accumulate on polymeric solid phases instead of being soluble in the aqueous phase.⁶⁸ According to Log K_{ow} values of phenolic compounds, (E)-Anethol (Log $K_{ow} = 3.4$) is the most hydrophobic, followed by P-chlorobenzoic acid (Log $K_{ow} = 2.65$). On the contrary, hydroxytyrosol (Log $K_{ow} = -0.7$) and tyrosol (Log $K_{ow} = 0.04$) are the most hydrophilic compounds, which are difficult to be extracted from water because of their strong interactions with the molecules of water via H-bonding. In order to fully remove these pollutants from water, the sorbent phases have to establish stronger interactions with hydroxytyrosol and tyrosol.

Hence, we studied the performance of these polymers to adsorb simultaneously eleven polyphenols in aqueous solutions and the impact of their varied chemical structure on the adsorption efficiency of polar pollutants. The adsorption efficiency of phenolic compounds after different times (1, 3, 5 and 24 h) for the PEPTs based on monomer (6) (**P1**, **P2**) and on monomer (7) (**P3**, **P4**) are presented respectively in Tables 8 and 9.

Table 8: Adsorption capacity (%) of benzene derivatives on polymers P1 and P2.

Time (hours)	1		3		5		24	
Polymers	P1	P2	P1	P2	P1	P2	P1	P2
Benzene Derivatives	Adsorption (%)							
Hydroxytyrosol	5	13	8	17	9	21	13	27
Tyrosol	9	20	13	23	17	30	20	45
4-hydroxybenzoic acid	18	33	24	47	27	79	29	100
Caffeic acid	20	36	26	50	29	89	35	100
Ferulic acid	31	56	51	80	60	100	64	100
Benzoic acid	39	58	44	71	65	100	70	100
P-Anisic acid	58	63	74	86	82	100	88	100
P-Toluic acid	46	80	69	87	85	100	90	100
P-Chlorobenzoic acid	68	84	84	100	90	100	92	100
Eugenol	85	92	95	100	99	100	100	100
(E)-Anethol	100	100	100	100	100	100	100	100

Adsorption results for polymers P1 and P2 obtained from monomer (6), showed that the polymer P1 obtained from BPA display interesting sorption properties during the first hour of contact for (E)-anethol (100%), eugenol (85%) and P-chlorobenzoic acid (68%) due to their hydrophobicity. In contrast, this polymer exhibited lower adsorption efficiency towards

hydrophilic pollutants such as hydroxytyrosol (5%), tyrosol (9%) and 4-hydroxybenzoic acid (18%). Hydrophobic interactions between the non-polar compounds and polymer P1 are expected to dominate in aqueous systems. Comparing the values obtained for P1 and polymer P2, a slight increase of adsorption efficiency was observed for hydrophilic and hydrophobic compounds. This increase was mainly related to the introduction of isosorbide unit in the polymer P2, which is known to be responsive of the hydrophilic characters of the polymer. Indeed, after 24 h most of the phenols were completely adsorbed by polymer P2, with the exception of hydroxytyrosol and tyrosol whose adsorption efficiency remains low (27% and 45 %) even after 24 h of contact. The sorption results showed that the biosourced P2 used is not able to establish strong enough interactions with these high polar pollutants.

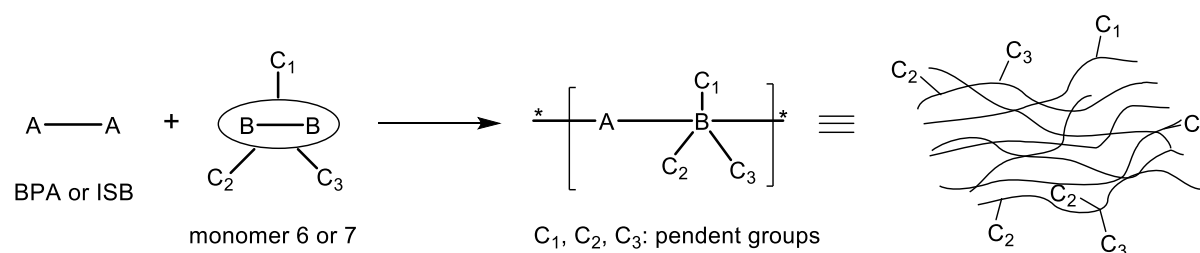
For the adsorption on monomer (7)-based polymers (Table 9), the polymer P3, shows higher percent of adsorption in comparison with polymers P1 and P2 derived from monomer (6). It was found that after one hour of contact, with polymer P3 45% of hydroxytyrosol (Table 9) was adsorbed whereas 5 % and 13 % was retained by P1 and P2, respectively. This finding can be explained by the difference in the chemical structure of this polymer, which contains hydrophilic hydroxyl groups as pendants chains, contributing as well to other hydrogen bonds interactions between polymer P3 and micropollutants. The important increase in the adsorption efficiency of benzene derivatives observed with polymer P3 is due to these additional interactions. For the bio-based polymer P4, we clearly note that this polymer exhibits very high sorption efficiency (87-100 % after 3 h) and then increased slightly until 93-100% for all pollutants after 24 h. This is another confirmation that isosorbide group make bio-based polymers much more hydrophilic which increases their tendency to remove polar pollutants in water. The low-polarity compound was adsorbed via π - π interactions, whereas polar pollutant prefer to bond with active functional groups of polymer P4. Hydroxyl and carboxyl groups of pollutant form intermolecular hydrogen bonds with hydroxyl groups and oxygen and nitrogen atoms in the polymer.

The adsorption results of phenolic compounds on polymers P1-P4 indicate that the hydrophilicity of polymers (presence of oxygen and nitrogen functional groups) plays an important role in the adsorption capacity of polar micropollutants on polymers. The adsorption was increased with increasing polymer hydrophilicity.

Table 9: Adsorption efficiency (%) of benzene derivatives on polymers P3 and P4.

Time (hours)	1		3		5		24	
Polymers	P3	P4	P3	P4	P3	P4	P3	P4
Benzene Derivatives	Adsorption (%)							
Hydroxytyrosol	45	78	47	87	51	91	55	93
Tyrosol	50	85	55	90	60	96	64	97
4-hydroxybenzoic acid	71	99	83	100	85	100	100	100
Caffeic acid	65	97	86	100	86	100	100	100
Ferulic acid	82	99	89	100	92	100	100	100
Benzoic acid	85	100	91	100	83	100	100	100
P-Anisic acid	90	100	92	100	93	100	100	100
P-Toluic acid	94	100	95	100	96	100	100	100
P-Chlorobenzoic acid	96	100	100	100	100	100	100	100
Eugenol	95	100	100	100	100	100	100	100
(E)-Anethol	100	100	100	100	100	100	100	100

According to these results, the incorporation of 1,2,3-triazole groups as pendent chains in the backbone of poly(ether-pyridine)s can be considered as an important parameter, that can affect the adsorption efficiency of the polymers. In our work, the fluorinated monomers 6 and 7 (B-B) used for the elaboration of novel adsorbents presented three pendent groups in their main chains, including morpholine group (C₁) and two triazole units (C₂ and C₃) (Figure 10).

**Figure 10. Representative scheme of resulting polymers with effects of entanglements and pendent group structures.**

In fact, these pendent groups precisely 1,2,3-triazoles can form an attractive polar cavity for the trapping of hydrophilic pollutants from water. The cavity has a Lewis base character and the nitrogen atoms at the 2 and 3 positions of triazole can act as hydrogen-bond acceptors, then the phenols are expected to be retained into this cavity (Figure 11).

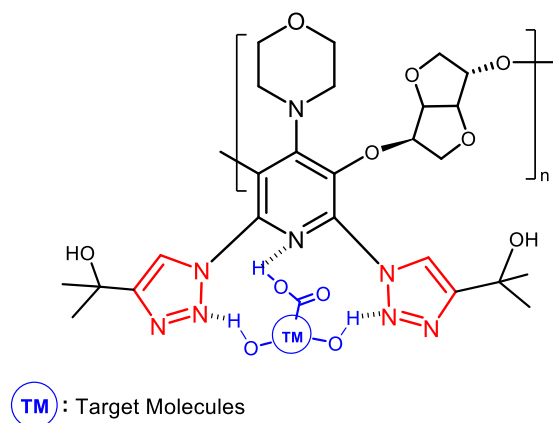
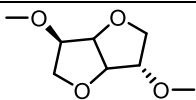
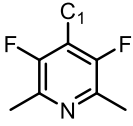
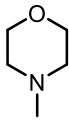
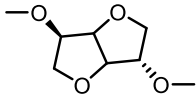
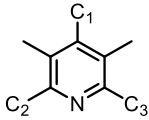
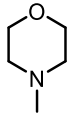
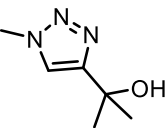


Figure 11. Possible adsorption mechanism involved in adsorption of target molecules onto the polymers.

The obtained maximum adsorption efficiency of 4-hydroxybenzoic acid by P4 after 1 h of contact was compared to reported literature (Table 10).

Table 10. Comparison of maximum adsorption capacity of 4-hydroxybenzoic acid into PEPT (after 1h of contact) with reported adsorbents.

Adsorbents		Adsorption efficiency after 1 h (%)	References
Polyethersulfone	A	80	[69]
	B		
	C ₁ , C ₂ , C ₃		
Polyetherpyridine from 2,6-difluoropyridine	A	95	[70]
	B		
	C ₁		
	C ₂		

	C ₃	-		
Polyetherpyridine from pentafluoropyridine	A		93	[51]
	B			
	C ₁			
	C ₂ , C ₃	-		
Polyether-pyridine from pentafluoropyridine containing triazole groups	A		99	This work
	B			
	C ₁			
	C ₂ , C ₃			

As shown in Table 10, it appears that the linear polyethersulfone without pendent groups presents the lower sorption efficiency (80%) for 4-hydroxybenzoic acid. For the polyetherpyridines, the introduction of pendent groups clearly enhanced their affinity for this pollutant (>93%). For instance, these groups make our polymer P4 efficient adsorbent for 4-hydroxybenzoic acid (99%) as well as for more hydrophilic phenolic compounds like hydroxytyrosol and tyrosol.

4. Conclusion

This study was carried out to synthesize innovative poly(ether-pyridine)s containing 1,2,3-triazoles groups in order to be used as adsorbents of phenolic compounds from water. These polymers were successfully prepared by polycondensation of two novel 1,2,3-triazole-based fluorinated monomers derived from pentafluoropyridine with isosorbide and bisphenol A diols. Their chemical structures were confirmed by ¹H, ¹⁹F NMR and MALDI-TOF mass spectrometry. These polymers were characterized by TGA and DSC analysis. They have been

then evaluated for the adsorption of eleven polyphenols from water. The results of sorption showed that the polymer P4, based on isosorbide with hydroxyl groups as pendent chains, presented the highest adsorption efficiency of hydrophilic pollutants. This indicated that the incorporation of pendent groups in the backbone of polymers plays a major role in the increases of the adsorption capacity of linear polymers.

Funding: We would like to acknowledge the financial support of CAMPUS-FRANCE and the French Embassy in Tunisia (Dr. Pierre Durand de Ramefort) for the SSHN grant, of the POLYAM project, of the High Ministry of Education and Research in Tunisia for doctoral grant. Region Auvergne Rhone Alpes is acknowledged for the Pack Ambition International Project, EMBAI #246413. CNRS is acknowledged for the IRP NARES. The research leading to these results has received funding from the European Union Horizon 2020 (TUNTWIN) research and innovation program under grant agreement n° 952306. The authors acknowledge the financial support of the EU H2020 WIDESPREAD Program entitled Bionanosens grant agreement # 951887.

References

- [1] Edwards CA. Factors affecting the persistence of pesticides in the soil. *Chem Ind Lond*, 1974.
- [2] Sheets TJ. Metabolism of herbicides, review of disappearance of substituted urea herbicides from soil. *J Agric Food Chem*, 1964, 12:30-33. doi: [10.1021/jf60131a009](https://doi.org/10.1021/jf60131a009)
- [3] Goerlitz DF, Troutman DE, Godsy EM., *et al.* Migration of wood-preserving chemicals in contaminated groundwater in a sand aquifer at Pensacola, Florida. *Environ Sci Technol*, 1985, 19:955-961. doi : [10.1021/es00140a012](https://doi.org/10.1021/es00140a012)
- [4] McCarthy J, Zachara J. ES&T Features: Subsurface transport of contaminants. *Environ Sci Technol*, 1989, 23:496-502. doi : [10.1021/es00063a602](https://doi.org/10.1021/es00063a602)
- [5] Schwarzenbach RP, Giger W, Hoehn E., *et al.* Behavior of organic compounds during infiltration of river water to groundwater. Field studies. *Environ Sci Technol*, 1983, 17:472-479. doi: [10.1021/es00114a007](https://doi.org/10.1021/es00114a007)
- [6] Schwarzenbach RP, Escher BI, Fenner K., *et al.* The challenge of micropollutants in aquatic systems. *Science*, 2006, 313:1072-1077. doi: [10.1126/science.1127291](https://doi.org/10.1126/science.1127291)
- [7] Richardson SD, Ternes TA. Water analysis: emerging contaminants and current issues. *Anal Chem*, 2014, 86:2813-2848. doi: [10.1021/ac500508t](https://doi.org/10.1021/ac500508t)
- [8] Murray KE, Thomas SM, Bodour AA. Prioritizing research for trace pollutants and emerging contaminants in the freshwater environment. *Environ Pollut*, 2010, 158:3462-3471. doi : [10.1016/j.envpol.2010.08.009](https://doi.org/10.1016/j.envpol.2010.08.009)
- [9] Mckinlay R, Plant JA, Bell JNB., *et al.* Endocrine disrupting pesticides: implications for risk assessment. *Environ Int*, 2008, 34:168-183. doi: [10.1016/j.envint.2007.07.013](https://doi.org/10.1016/j.envint.2007.07.013)
- [10] Daughton CG, Ternes TA. Pharmaceuticals and personal care products in the environment: agents of subtle change. *Environ Health Perspect*, 1999, 107:907-938. doi : [10.1289/ehp.99107s6907](https://doi.org/10.1289/ehp.99107s6907)
- [11] Robinson T, McMullan G, Marchant R., *et al.* Remediation of dyes in textile effluent: a critical review on current treatment technologies with a proposed alternative. *Bioresour Technol*, 2001, 77:247-255. doi: [10.1016/S0960-8524\(00\)00080-8](https://doi.org/10.1016/S0960-8524(00)00080-8)
- [12] Fu Y, Viraraghavan T. Fungal decolorization of dye wastewaters: a review. *Bioresour Technol*, 2001, 79:251-262. doi: [10.1016/S0960-8524\(01\)00028-1](https://doi.org/10.1016/S0960-8524(01)00028-1)
- [13] Chern JM, Wu CY. Desorption of dye from activated carbon beds: effects of temperature, pH, and alcohol. *Water Res*, 2001, 35: 4159-4165. doi: [10.1016/S0043-1354\(01\)00127-0](https://doi.org/10.1016/S0043-1354(01)00127-0)
- [14] Pérez M, Torrades F, Domènech X., *et al.* Fenton and photo-Fenton oxidation of textile effluents. *Water Res*, 2002, 36:2703-2710. doi: [10.1016/S0043-1354\(01\)00506-1](https://doi.org/10.1016/S0043-1354(01)00506-1)
- [15] An H, Qian Y, Gu X., *et al.* Biological treatment of dye wastewaters using an anaerobic-oxic system. *Chemosphere*, 1996, 33:2533-2542. doi: [10.1016/S0045-6535\(96\)00349-9](https://doi.org/10.1016/S0045-6535(96)00349-9)
- [16] Ho YS, McKay G. Sorption of dye from aqueous solution by peat. *Chem Eng J*, 1998, 70:115-124. doi: [10.1016/S0923-0467\(98\)00076-1](https://doi.org/10.1016/S0923-0467(98)00076-1)

- [17] Dąbrowski A. Adsorption-from theory to practice. *Adv Colloid Interface Sci*, 2001, 93:135-224. doi: [10.1016/S0001-8686\(00\)00082-8](https://doi.org/10.1016/S0001-8686(00)00082-8)
- [18] Órfão J.J.M, Silva A.I.M, Pereira J.C.V., *et al.* Adsorption of a reactive dye on chemically modified activated carbons-influence of pH. *J Colloid Interface Sci*, 2006, 296:480-489. doi: [10.1016/j.jcis.2005.09.063](https://doi.org/10.1016/j.jcis.2005.09.063)
- [19] Putra EK, Pranowo R, Sunarso J., *et al.* Performance of activated carbon and bentonite for adsorption of amoxicillin from wastewater: Mechanisms, isotherms and kinetics. *Water Res*, 2009, 43:2419-2430. doi: [10.1016/j.watres.2009.02.039](https://doi.org/10.1016/j.watres.2009.02.039)
- [20] Kovalova L, Knappe DRU, Lehnberg K., *et al.* Removal of highly polar micropollutants from wastewater by powdered activated carbon. *Environ Sci Pollut Res*, 2013, 20:3607-3615. doi: [10.1007/s11356-012-1432-9](https://doi.org/10.1007/s11356-012-1432-9)
- [21] Chiang PC, Chang EE, Wu JS. Comparison of chemical and thermal regeneration of aromatic compounds on exhausted activated carbon. *Water Sci Technol*, 1997, 35: 279-285. doi: [10.2166/wst.1997.0287](https://doi.org/10.2166/wst.1997.0287)
- [22] San Miguel G, Lambert SD, Graham N.J.D. The regeneration of field-spent granular-activated carbons. *Water Res*, 2001, 35: 2740-2748. doi: [10.1016/S0043-1354\(00\)00549-2](https://doi.org/10.1016/S0043-1354(00)00549-2)
- [23] Wang S, Boyjoo Y, Choueib A., *et al.* Removal of dyes from aqueous solution using fly ash and red mud. *Water Res*, 2005, 39:129-138. doi: [10.1016/j.watres.2004.09.011](https://doi.org/10.1016/j.watres.2004.09.011)
- [24] Synowiecki J, Al-khateeb NA. Production, properties, and some new applications of chitin and its derivatives. *Crit Rev Food Sci Nutr*, 2003, 43:145-171. doi: [10.1080/10408690390826473](https://doi.org/10.1080/10408690390826473)
- [25] Kumar M.N.R. A review of chitin and chitosan applications. *React Funct Polym*, 2000, 46:1-27. doi: [10.1016/S1381-5148\(00\)00038-9](https://doi.org/10.1016/S1381-5148(00)00038-9)
- [26] Bailey SE, Olin TJ, Bricka RM., *et al.* A review of potentially low-cost sorbents for heavy metals. *Water research*, 1999, 33:2469-2479. doi: [10.1016/S0043-1354\(98\)00475-8](https://doi.org/10.1016/S0043-1354(98)00475-8)
- [27] Yuryev VP, Cesaro A, Bergthaller WJ. Starch and Starch Containing Origins: Structure, Properties and New Technologies. *Nova Publisher*, 2002.
- [28] Wurzburg OB. Modified starches-properties and uses, CRC Press, Boca Raton, 1986, 18-41
- [29] Sandford PA, Baird J. Industrial utilization of polysaccharides. In *The polysaccharides*, Ed Aspinall GO, Academic Press, New-York, 1983, 411-490. doi: [10.1016/B978-0-12-065602-8.50012-1](https://doi.org/10.1016/B978-0-12-065602-8.50012-1)
- [30] Babel S, Kurniawan TA. Low-cost adsorbents for heavy metals uptake from contaminated water: a review. *J Hazard Mater*, 2003, 97:219-243. doi: [10.1016/S0304-3894\(02\)00263-7](https://doi.org/10.1016/S0304-3894(02)00263-7)
- [31] Varma AJ, Deshpande SV, Kennedy JF. Metal complexation by chitosan and its derivatives: a review. *Carbohydr Polym*, 2004, 55:77-93. doi: [10.1016/j.carbpol.2003.08.005](https://doi.org/10.1016/j.carbpol.2003.08.005)
- [32] Singh M, Sharma R, Banerjee UC. Biotechnological applications of cyclodextrins. *Biotechnol Adv*, 2002, 20:341-359. [10.1016/S0734-9750\(02\)00020-4](https://doi.org/10.1016/S0734-9750(02)00020-4)
- [33] Crini G, Morcellet M. Synthesis and applications of adsorbents containing cyclodextrins. *J Sep Sci*, 2002, 25:789-813. doi: [10.1002/1615-9314\(20020901\)25:13<789::AID-JSSC789>3.0.CO;2-J](https://doi.org/10.1002/1615-9314(20020901)25:13<789::AID-JSSC789>3.0.CO;2-J)
- [34] Del Valle EM. Cyclodextrins and their uses: a review. *Process Biochem*, 2004, 39:1033-1046. doi: [10.1016/S0032-9592\(03\)00258-9](https://doi.org/10.1016/S0032-9592(03)00258-9)
- [35] Alsaiee A, Smith BJ, Xiao L., *et al.* Rapid removal of organic micropollutants from water by a porous β -cyclodextrin polymer. *Nature*, 2016, 529:190-194. doi: [10.1038/nature16185](https://doi.org/10.1038/nature16185)
- [36] Lu P, Cheng J, Li Y., *et al.* Novel porous β -cyclodextrin/pillar [5] arene copolymer for rapid removal of organic pollutants from water. *Carbohydr Polym*, 2019, 216:149-156. doi : [10.1016/j.carbpol.2019.04.015](https://doi.org/10.1016/j.carbpol.2019.04.015)
- [37] Paspirgelyte R, Grazulevicius JV, Grigalevicius S., *et al.* N, N'-Diphenyl-1, 4-phenylenediamine-based enamines containing reactive functional groups as building blocks for electro-active polymers. *Des Monomers Polym*, 2009, 12:579-587. doi: [10.1163/138577209X12519685854626](https://doi.org/10.1163/138577209X12519685854626)
- [38] Okada M, Tachikawa K, Aoi K. Biodegradable polymers based on renewable resources. II. Synthesis and biodegradability of polyesters containing furan rings. *J Polym Sci Part A: Polym Chem*, 1997, 35:2729-2737. doi: [10.1002/\(SICI\)1099-0518\(19970930\)35:13<2729::AID-POLA18>3.0.CO;2-D](https://doi.org/10.1002/(SICI)1099-0518(19970930)35:13<2729::AID-POLA18>3.0.CO;2-D)
- [39] Storbeck R, Rehahn M, Ballauff M. Synthesis and properties of high-molecular-weight polyesters based on 1, 4: 3, 6-dianhydrohexitols and terephthalic acid. *Makromol Chem*, 1993,194:53-64. doi : [10.1002/macp.1993.021940104](https://doi.org/10.1002/macp.1993.021940104)
- [40] Majdoub M, Loupy A, Flèche G. Nouveaux polyéthers et polyesters à base d'isorbide: synthèse et caractérisation. *Eur Polym J*, 1994, 30:1431-1437. doi : [10.1016/0014-3057\(94\)90274-7](https://doi.org/10.1016/0014-3057(94)90274-7)
- [41] Chatti S, Bortolussi M, Bogdal D., *et al.* Microwave-assisted polycondensation of aliphatic diols of isorbide with aliphatic disulphonylestere via phase-transfer catalysis. *Eur Polym J*, 2004, 40:561-577. doi : [10.1016/j.eurpolymj.2003.10.027](https://doi.org/10.1016/j.eurpolymj.2003.10.027)

- [42] Caouthar AA., Loupy A, Bortolussi M., *et al.* Synthesis and characterization of new polyamides based on diphenylaminoisobornide. *J Polym Sci Part A: Polym Chem*, 2005, 43:2480-2491. doi: [10.1002/pola.21116](https://doi.org/10.1002/pola.21116)
- [43] Caouthar A, Roger P, Tessier M., *et al.* Synthesis and characterization of new polyamides derived from di (4-cyanophenyl) isobornide. *Eur Polym J*, 2007, 43:220-230. doi: [10.1016/j.eurpolymj.2006.08.012](https://doi.org/10.1016/j.eurpolymj.2006.08.012)
- [44] Yokoe M, Aoi K, Okada M. Biodegradable polymers based on renewable resources VIII. Environmental and enzymatic degradability of copolycarbonates containing 1, 4: 3, 6-dianhydrohexitols. *J Appl Polym Sci*, 2005, 98:1679-1687. doi: [10.1002/app.22339](https://doi.org/10.1002/app.22339)
- [45] Chatti S, Schwarz G, Kricheldorf HR. Cyclic and noncyclic polycarbonates of isobornide (1, 4: 3, 6-dianhydro-D-glucitol). *Macromolecules*, 2006, 39: 9064-9070. doi: [10.1021/ma0606051](https://doi.org/10.1021/ma0606051)
- [46] Besset C, Binauld S, Ibert M., *et al.* Copper-catalyzed vs thermal step growth polymerization of starch-derived α -azide- ω -alkyne dianhydrohexitol stereoisomers: to click or not to click. *Macromolecules*, 2010, 43:17-19. doi: [10.1021/ma9024784](https://doi.org/10.1021/ma9024784)
- [47] Besset C, Pascual JP, Fleury E., *et al.* Structure-properties relationship of biosourced stereocontrolled polytriazoles from click chemistry step growth polymerization of diazide and dialkyne dianhydrohexitols. *Biomacromolecules*, 2010, 11:2797-2803. doi: [10.1021/bm100872h](https://doi.org/10.1021/bm100872h)
- [48] Chatti S., Hani MA, *High Perform Polym*, 2009, 21:105-118. doi: [10.1177/0954008308088296](https://doi.org/10.1177/0954008308088296)
- [49] Abderrazak HB, Fildier A, Romdhane HB., *et al.* Synthesis of new poly (ether ketone) s derived from biobased diols. *Macromol Chem Phys*, 2013, 214:1423-1433. [10.1002/macp.201300015](https://doi.org/10.1002/macp.201300015)
- [50] Casabianca H, Chatti, S, Mercier R. Use of a polymer containing units derived from 1,4,3,6 dianhydro-d-hexitol for adsorbing chemical compounds. 2019. France, N° de brevet: FR 3074806
- [51] Gomri M, Abderrazak H, Chabbah T., *et al.* Adsorption characteristics of aromatic pollutants and their halogenated derivatives on bio-based poly (ether-pyridine)s. *J Environ Chem Eng*, 2020, 8:104-333. doi: [10.1016/j.jece.2020.104333](https://doi.org/10.1016/j.jece.2020.104333)
- [52] Purcell WP, Singer JA. Electronic and molecular structure of selected unsubstituted and dimethyl amides from measurements of electric moments and nuclear magnetic resonance. *J Phys Chem*, 1967, 71:4316-4319. doi: [10.1021/j100872a024](https://doi.org/10.1021/j100872a024)
- [53] Bazzar M, Ghaemy M, Alizadeh R. Novel fluorescent light-emitting polymer composites bearing 1, 2, 4-triazole and quinoxaline moieties: Reinforcement and thermal stabilization with silicon carbide nanoparticles by epoxide functionalization. *Polym Degrad Stab*, 2012, 97:1690-1703. doi: [10.1016/j.polymdegradstab.2012.06.018](https://doi.org/10.1016/j.polymdegradstab.2012.06.018)
- [54] Bazzar M, Ghaemy M, Alizadeh R. Synthesis and characterization of new fluorescent polyimides bearing 1, 2, 4-triazole and 1, 2-diaryl quinoxaline: study properties and application to the extraction/elimination of metallic ions from aqueous media. *React Funct Polym*, 2013, 73:492-498. doi: [10.1016/j.reactfunctpolym.2012.11.009](https://doi.org/10.1016/j.reactfunctpolym.2012.11.009)
- [55] Ghaemy M, Qasemi S, Ghassemi K., *et al.* Nanostructured composites of poly (triazole-amide-imide) s and reactive titanium oxide by epoxide functionalization: thermal, mechanical, photophysical and metal ions adsorption properties. *J Polym Res*, 2013, 20:1-15. doi: [10.1007/s10965-013-0278-2](https://doi.org/10.1007/s10965-013-0278-2)
- [56] Rostovtsev VV, Green LG, Fokin VV., *et al.* A stepwise Huisgen cycloaddition process: copper (I)-catalyzed regioselective "ligation" of azides and terminal alkynes. *Angew Chem Int Ed Engl*, 2002, 114:2708-2711. doi: [10.1002/1521-3773\(20020715\)41:14<2596::AID-ANIE2596>3.0.CO;2-4](https://doi.org/10.1002/1521-3773(20020715)41:14<2596::AID-ANIE2596>3.0.CO;2-4)
- [57] Tornøe CW, Christensen C, Meldal M. Peptidotriazoles on solid phase:[1, 2, 3]-triazoles by regioselective copper (I)-catalyzed 1, 3-dipolar cycloadditions of terminal alkynes to azides. *J Org Chem*, 2002, 67:3057-3064. doi: [10.1021/jo011148j](https://doi.org/10.1021/jo011148j)
- [58] Wu H, Li H, Kwok RTK *et al.* A recyclable and reusable supported Cu (I) catalyzed azide-alkyne click polymerization. *Sci Rep*, 2014, 4:1-5. doi: [10.1038/srep05107](https://doi.org/10.1038/srep05107)
- [59] Chambers RD, Sargent CR. Polyfluoroheteroaromatic compounds. *Adv Heterocycl Chem*. 1981, 28:1-71. doi: [10.1016/S0065-2725\(08\)60040-9](https://doi.org/10.1016/S0065-2725(08)60040-9)
- [60] Brooke GM. The preparation and properties of polyfluoro aromatic and heteroaromatic compounds. *J Fluor Chem*, 1997, 86:1-76. doi: [10.1016/S0065-2725\(08\)60040-9](https://doi.org/10.1016/S0065-2725(08)60040-9)
- [61] Anku WW, Mamo MA, Govender PP. Phenolic compounds in water: sources, reactivity, toxicity and treatment methods. In Phenolic compounds, Ed Soto-Hernandez M, Palma-Tenango M, del Rosario M, IntechOpen, 2017, 419-443. doi: [10.5772/66927](https://doi.org/10.5772/66927)
- [62] Podolan G, Jungk P, Lentz D., *et al.* Studies on the Synthesis of Specifically Fluorinated 4-Amino-pyridine Derivatives by Regioselective Nucleophilic Aromatic Substitution and Catalytic Hydrodefluorination. *Adv Synth Catal*, 2015, 357:3215-3228. doi: [10.1002/adsc.201500393](https://doi.org/10.1002/adsc.201500393)
- [63] Banks RE., Burgess JE, Cheng WM., *et al.* 93. Heterocyclic polyfluoro-compounds. Part IV. Nucleophilic substitution in pentafluoropyridine: the preparation and properties of some 4-substituted 2, 3, 5, 6-tetrafluoropyridines. *J Chem Soc (Resumed)*, 1965, 575-581. doi: [10.1039/jr9650000575](https://doi.org/10.1039/jr9650000575)
- [64] Chambers RD, Hutchinson J, Musgrave W.K.R. 722. Polyfluoro-heterocyclic compounds. Part II. Nucleophilic substitution in pentafluoropyridine. *J Chem Soc (Resumed)*, 1964, 3736-3739. doi: [10.1039/jr9640003736](https://doi.org/10.1039/jr9640003736)

- [65] Bakherad M, Ghalenoei AK, Keivanloo A. Synthesis of 1, 4-Disubstituted 1, 2, 3-Triazoles via 1, 3-Dipolar Cycloaddition/C–N Coupling of Propargyl Alcohols/amines and Aryl Azides. *J Heterocycl Chem*, 2018, 55:2683-2692. doi: [10.1002/jhet.3325](https://doi.org/10.1002/jhet.3325)
- [66] Belgacem C, Medimagh R, Kricheldorf H., *et al.* Copolyethersulfones of 1, 4: 3, 6-dianhydrohexitols and bisphenol A. *Des Monomers Polym*, 2016, 19:248-255. doi: [10.1080/15685551.2015.1136531](https://doi.org/10.1080/15685551.2015.1136531)
- [67] Chabbah T, Abderrazak H, Souissi R., *et al.* A Sensitive Impedimetric Sensor Based on Biosourced Polyphosphine Films for the Detection of Lead Ions. *Chemosensors*, 2020, 8:34. doi: [10.3390/chemosensors8020034](https://doi.org/10.3390/chemosensors8020034)
- [68] Schäfer AI, Akanyeti I, Semião AJ. Micropollutant sorption to membrane polymers: a review of mechanisms for estrogens. *Adv Colloid Interface Sci*, 2011, 164:100-117. doi: [10.1016/j.cis.2010.09.006](https://doi.org/10.1016/j.cis.2010.09.006)
- [69] Chabbah T, Abderrazak H, Saint martin P., *et al.* Synthesis of Glux based polymers for removal of benzene derivatives and pesticides from water. *Polym Adv Technol*, 2020, 31:2339-2350. doi: [10.1002/pat.4953](https://doi.org/10.1002/pat.4953)
- [70] Jlalia I, Chabbah T, Chatti S., *et al.* Alternating bio-based pyridinic copolymers modified with hydrophilic and hydrophobic spacers as sorbents of aromatic pollutants. *Polym Adv Technol*, 2022, 33:1057-1068. doi: [10.1002/pat.5578](https://doi.org/10.1002/pat.5578)